N-terminal truncation of Lats1 causes abnormal cell growth control and chromosomal instability

Norikazu Yabuta[1,*], Satomi Mukai[1,*], Ayumi Okamoto[1], Daisuke Okuzaki[1,2], Hirokazu Suzuki[1], Kosuke Torigata[1], Kaori Yoshida[1], Nobuhiro Okada[1,‡], Daisaku Miura[3], Akihiko Ito[4], Masahito Ikawa[5], Masaru Okabe[5] and Hiroshi Nojima[1,2,§]

[1]Department of Molecular Genetics, Osaka University, 3-1 Yamadaoka, Suita City, Osaka 565-0871, Japan
[2]DNA-chip Development Center for Infectious Diseases, Research Institute for Microbial Diseases, Osaka University, 3-1 Yamadaoka, Suita City, Osaka 565-0871, Japan
[3]Department of Pharmacy, Hyogo University of Health Sciences, 1-3-6 Minatojima, Chuo-ku, Kobe city, Hyogo 650-8530, Japan
[4]Department of Pathology, Kinki University Faculty of Medicine, 377-2 Ohno-Higashi, Osaka-Sayama, Osaka 589-8511, Japan
[5]Genome Information Research Center, Osaka University, 3-1 Yamadaoka, Suita City, Osaka 565-0871, Japan

*These authors contributed equally to this work
‡Present address: Division of Cellular and Developmental Biology, Molecular and Cell Biology Department, University of California at Berkeley, Berkeley, CA 94705, USA
§Author for correspondence (snj-0212@biken.osaka-u.ac.jp)

Accepted 21 November 2012
Journal of Cell Science 126, 508–519

doi: 10.1242/jcs.113431

Summary

The tumor suppressors Lats1 and Lats2 are mediators of the Hippo pathway that regulates tissue growth and proliferation. Their N-terminal non-kinase regions are distinct except for Lats conserved domains 1 and 2 (LCD1 and LCD2), which may be important for Lats1/2-specific functions. Lats1 knockout mice were generated by disrupting the N-terminal region containing LCD1 ($Lats1^{\Delta N/\Delta N}$). Some $Lats1^{\Delta N/\Delta N}$ mice were born safely and grew normally. However, mouse embryonic fibroblasts (MEFs) from $Lats1^{\Delta N/\Delta N}$ mice displayed mitotic defects, centrosomal overduplication, chromosomal misalignment, multipolar spindle formation, chromosomal bridging and cytokinesis failure. They also showed anchorage-independent growth and continued cell cycles and cell growth, bypassing cell-cell contact inhibition similar to tumor cells. $Lats1^{\Delta N/\Delta N}$ MEFs produced tumors in nude mice after subcutaneous injection, although the tumor growth rate was much slower than that of ordinary cancer cells. Yap, a key transcriptional coactivator of the Hippo pathway, was overexpressed and stably retained in $Lats1^{\Delta N/\Delta N}$ MEFs in a cell density independent manner, and *Lats2* mRNA expression was downregulated. In conclusion, N-terminally truncated Lats1 induced Lats2 downregulation and Yap protein accumulation, leading to chromosomal instability and tumorigenesis.

Key words: Lats1, Hippo, Lats2, YAP, Chromosome instability

Introduction

Aberrant cell growth and chromosomal instability (CIN), two major hallmarks of human malignant cancer cells (Hanahan and Weinberg, 2011; Gordon et al., 2012), are caused by malfunctions of the machineries that regulate various cell growth control signaling pathways, cell cycle, and cell death. These machineries and their related molecules may be potent and promising cancer therapy targets.

The Hippo pathway, a novel tumor suppressor signaling pathway that regulates cell growth, organ size, and stem cell self-renewal, is conserved in fruit flies and higher eukaryotes (Pan, 2010; Zhao et al., 2011). The core pathway in mammalian cells consists of the Ste20-like Ser/Thr kinases, Mst1/2 (mammalian sterile 20-like kinase 1 and 2, as Hippo homologues), the Dbf2-related Ser/Thr kinases, Lats1/2 (large tumor suppressor 1 and 2, as Warts homologues), their adaptor proteins, hWW45 (as a Salvador homologue) and Mob1 (Mps one-binder 1, as a Mats homologue), and the transcriptional coactivators Yap/Taz (yes-associated protein and transcriptional coactivator with PDZ-binding motif, as Yorkie homologues).

When the Hippo pathway is activated in response to upstream signals (e.g. cell-cell contact), Mst1/2 kinases phosphorylate and activate Lats1/2 kinases, which phosphorylate Yap/Taz and prevent their nuclear translocation to promote transcription of cell-proliferative and anti-apoptotic genes. The Lats-mediated negative regulation of Taz is mediated through a similar mechanism (Liu et al., 2010). When the Hippo pathway signaling is turned off, the inhibitory phosphorylation of Yap/Taz is cancelled. These proteins enter the nucleus, where they associate with and activate transcription factors, such as those of the Tead (TEA domain transcription factor, as Scalloped homologue) family, thereby inducing the expression of cell-proliferative and anti-apoptotic genes (Zhao et al., 2008).

The Hippo core pathway is tightly regulated by various upstream factors, including Fat1/4, Merlin/Nf2, Kibra, Tao-1/TAOK, Willin/FRMD6 and Rassf, and some direct modulators of Lats1/2, including Ajuba, Itch and Angiomotin/Amot (Zhao et al., 2011; Boggiano and Fehon, 2012). Downregulation of Hippo pathway components such as Fat1/4, Merlin/Nf2, Kibra, Mst1/2 and Lats1/2, and overexpression of Yap/Taz occur in various human tumor cells because of epigenetic silencing or chromosome rearrangement; thus, this pathway probably has a functionally important role in human tumor suppression in breast, prostate, liver, and other organs (Pan, 2010). However, the detailed mechanisms of this pathway are not fully understood.

Lats1/2 kinases play pivotal roles in growth control through the Hippo pathway and in chromosomal stability through cell cycle checkpoint machinery (Visser and Yang, 2010). Lats1 or Lats2 overexpression induces cell cycle arrest, including G1/S and G2/M arrest, and apoptosis in human cancer cell lines (Yang et al., 2001; Xia et al., 2002; Kamikubo et al., 2003; Li et al., 2003; Ke et al., 2004). In particular, nuclear Lats2 directly binds to and inhibits Mdm2, an E3 ubiquitin ligase, in response to mitotic damage (e.g. treatment with spindle poisons), which in turn stabilizes p53 protein to prevent the accumulation of malignant cells with chromosomal instability (Aylon et al., 2006). Lats2 phosphorylates ASPP1 (apoptosis-stimulating protein of p53-1) in response to oncogenic stress, thereby triggering apoptosis through the p53-mediated induction of proapoptotic genes (Aylon et al., 2010). Interestingly, Lats1 also binds to and sequesters Mdm2, leading to p53 stabilization and apoptosis; however, unlike Lats2, Lats1 achieves these effects by mediating the Mst2-Rassf1A pathway (Matallanas et al., 2011).

Lats2 normally localizes to the centrosome, cytoplasm, and nucleus and regulates centrosomal integrity (Toji et al., 2004; Abe et al., 2006). Indeed, *Lats2*$^{-/-}$ knockout mouse embryonic fibroblasts (MEFs) reportedly exhibit centrosomal fragmentation [amplification of pericentriolar material (PCM) but not centrioles], abnormal mitotic spindle formation, chromosomal missegregation, and cytokinesis failure, leading to chromosomal instability (McPherson et al., 2004; Yabuta et al., 2007). Although Lats1 also localizes to the centrosome (Nishiyama et al., 1999), the kinase activity of overexpressed Lats1 or Lats2 does not appear to affect centrosomal duplication in human osteosarcoma U2OS cells, although enforced expression of Ndr1, a Lats1/2-related kinase, enhances centrosomal overduplication in a kinase activity-dependent manner (Hergovich et al., 2007). However, it remains unclear whether Lats1 helps to suppress centrosomal overduplication or fragmentation, because the centrosomal integrity in Lats1-deficient MEFs and -knockdown cell lines has not been reported. Furthermore, both Lats1/2 dynamically localize to chromosomes and the mitotic apparatus, including the central spindle, and regulate proper chromosome segregation, probably through the spindle assembly checkpoint, during mitotic progression and cytokinesis (Hirota et al., 2000; Iida et al., 2004; Yabuta et al., 2011). These studies suggest that Lats1/2 coordinate to prevent chromosomal instability by regulating the cell cycle and checkpoint machinery.

Mammalian and fruit fly homologues of Lats/Warts proteins possess a long, stretched N-terminal region located ~700 amino acids (aa) upstream of the conserved kinase domain (Visser and Yang, 2010). Because yeast homologues (budding yeast Dbf2/20 and fission yeast Sid2) do not possess this region, the N-terminal regions of Lats kinases may play an important role in tumor development and control of organ size. In fact, the N-terminal regions of Lats1/2 physically interact with various cell cycle regulators (Cdc2, Zyxin and LIMK1 for Lats1; Ajuba and Aurora-A for Lats2) and Hippo pathway regulators (Mob1, Yap, Taz and Kibra for Lats1/2). We, and others, showed that the N-terminal regions are phosphorylated by several kinases, including Cdc2/cyclin B (S613 of Lats1), NUAK1 (S464 of Lats1), PKCδ (S464 of Lats1), Aurora-A (S83 and S380 of Lats2) and Chk1/2 (S408 of Lats2), whereas the C-terminus is phosphorylated by Mst1/2 (S909 and T1079 of Lats1; S872 and T1041 of Lats2). These findings indicate that the N-terminal regions of Lats1/2 contribute to the physiological regulation of these proteins, including subcellular localization, protein stability, or enzymatic activity (Morisaki et al., 2002; Chan et al., 2005; Takahashi et al., 2006; Humbert et al., 2010; Okada et al., 2011; Yabuta et al., 2011).

The C-terminal regions of Lats1 and Lats2, including the kinase domain, are highly conserved (85% and 80% sequence identity in human and mouse, respectively). Their N-terminal halves share low similarity, except for two Lats conserved domains, LCD1 and LCD2 (Yabuta et al., 2000; Li et al., 2003). LCD1s [human Lats1, 12–167 amino acids (aa); Lats2, 1–160 aa] of Lats1/2 contain a UBA (ubiquitin-associated) domain, but LCD2s (Lats1, 458–523 aa; Lats2, 403–463 aa) do not. Deletion in either LCD1 or LCD2 of human Lats2 inhibits NIH3T3/*v-ras* cell growth and suppresses soft-agar colony formation, although Lats1 was not examined (Li et al., 2003). Thus, although the biological functions of LCDs are incompletely understood, the N-terminal regions of Lats1/2 appear to be functionally important for tumor suppression and kinase domain activity.

We generated knockout mice (*Lats1*$^{\Delta N/\Delta N}$) by disrupting exon 2 of the *Lats1* gene encoding the N-terminal region containing LCD1, but not LCD2. The goal was to investigate the physiological impact of the N-terminal region (especially LCD1) of Lats1 on cell growth, tumorigenicity, chromosome instability (e.g. centrosomal integrity), and Hippo pathway signaling. Although some *Lats1*$^{\Delta N/\Delta N}$ mice were safely born, the birth rate was very low and did not show Mendelian distribution. *Lats1*$^{\Delta N/\Delta N}$ MEFs expressing N-terminally truncated Lats1 protein exhibited drastic mitotic defects, including centrosomal overduplication, chromosomal missegregation, and cytokinesis failure. *Lats1*$^{\Delta N/\Delta N}$ MEFs showed abnormal cell growth, anchorage-independent growth, and Yap protein accumulation through downregulation of Lats2 expression in a cell density independent manner. These findings suggest that the N-terminal region of Lats1 is required for chromosomal stability and suppression of tumorigenicity through the regulation of Lats2 expression.

Results

Generation of knockout mice expressing N-terminally truncated Lats1 protein

St. John et al. previously reported a *Lats1* knockout mouse remaining exons encoding the 756-aa N-terminal region of mouse Lats1 (supplementary material Fig. S1A, top; St John et al., 1999). To investigate the physiological function of the N-terminal region (especially LCD1) of Lats1, we disrupted exon 2 (E2) of the mouse *Lats1* gene encoding the N-terminal region (1–117 aa), which contains LCD1 but not LCD2, replacing it with the neomycin-resistant cassette, PGK-neo (supplementary material Fig. S1A, bottom). Three independent 129/S2SvPas-derived mouse embryonic stem (ES) cell clones showed disruption of the N-terminus of *Lats1* (hereafter referred to as Lats1-ΔN), which was confirmed by genomic PCR using a specific primer pair (primers A and B) and Southern blot analysis using probe A (supplementary material Fig. S1B,C, clone #1B, 4A and 13B). Chimeric mice derived from these correctly targeted ES clones transmitted the germ-line mutation to their offspring. Homozygous C57BL/6 mice (*Lats1*$^{\Delta N/\Delta N}$) were obtained by intercrossing the heterozygous offspring, but the birth rate was very low (*Lats1*$^{+/+}$:*Lats1*$^{+/\Delta N}$:*Lats1*$^{\Delta N/\Delta N}$=35:44:13) and non-Mendelian. Mouse genotypes were confirmed by Southern blot analysis with probe A (supplementary material Fig. S1D) and by

genomic PCR with primers A-C (supplementary material Fig. S1E). Notably, *Lats1*$^{\Delta N/\Delta N}$ mice exhibited growth retardation and low body weight until 4 weeks after birth, but not thereafter (supplementary material Fig. S1F,G). These phenotypes are similar to those of C-terminally truncated Lats1 mice (St John et al., 1999). However, unlike St John's *Lats1* knockout mice, *Lats1*$^{\Delta N/\Delta N}$ mice did not develop tumors, such as soft-tissue sarcoma or ovarian stromal cell carcinoma, during the feeding period of about two years (data not shown). Thus, the loss of Lats1 activity might reduce tumor formation in *Lats1*$^{\Delta N/\Delta N}$ mice.

To elucidate mRNA expression of the Lats1-ΔN mutant in *Lats1*$^{\Delta N/\Delta N}$ mice, we designed seven primer pairs for RT-PCR (Fig. 1A). Pairs F1-R1, F2-R8, F3-R8, F4-R8, F5-R8, F6-R8 and F7-R7 were targeted to regions encoding the start-methionine (first Met^{1}) in E2 of mouse *Lats1*, the sixth internal Met^{118} in exon 3 (E3), the seventh internal Met^{141} in E3, the eighth internal Met^{151} in E3, the ninth internal Met^{163} in E3, the boundaries between E3 and exon 4 (E4), and part of E4, respectively. RT-PCR analyses using MEFs from *Lats1*$^{+/+}$ and *Lats1*$^{\Delta N/\Delta N}$ revealed that *Lats1* mRNA in *Lats1*$^{\Delta N/\Delta N}$ was transcribed from the region including the sixth internal Met^{118} in E3, because *Lats1* mRNA in *Lats1*$^{\Delta N/\Delta N}$ was expressed in all regions except those encoding the first Met^{1} in E2 (Fig. 1B).

Western blot analysis of MEF extracts using an anti-Lats1 antibody showed that smaller bands from the truncated Lats1 protein were additionally detected in *Lats1*$^{+/\Delta N}$ and *Lats1*$^{\Delta N/\Delta N}$, but not *Lats1*$^{+/+}$ MEFs (Fig. 1C). This finding suggests that *Lats1*$^{\Delta N/\Delta N}$ MEFs express N-terminally truncated, but not full-length, Lats1 protein, because the Lats1 antibody (clone #C66B5) recognizes amino acids surrounding Gly^{180} in human and mouse Lats1 (Fig. 1A). The Lats1-ΔN protein comprised ~1002–1042 aa. Thus, the sixth Met in E3 was likely used to generate the 1012-aa Lats1-ΔN protein in *Lats1*$^{\Delta N/\Delta N}$ MEFs. Moreover, we examined whether the Lats1-ΔN protein was expressed in embryos and/or adult mice of *Lats1*$^{+/\Delta N}$ and *Lats1*$^{\Delta N/\Delta N}$. Lats1-ΔN protein was expressed not only in MEFs but also in embryos at embryonic days 12.5 (E12.5) and 16.5 (E16.5), and in some adult mouse organs such as the liver, spleen and stomach (Fig. 1D,E).

Lats1$^{\Delta N/\Delta N}$ MEFs exhibit abnormal cell growth and anchorage-independent growth

LCD1 and LCD2 of Lats2 and its kinase activity are required for the inhibition of NIH3T3/*v-ras* cell growth and soft-agar colony formation (Li et al., 2003). However, the impact of the LCD regions of Lats1 on growth inhibition remains elusive. We

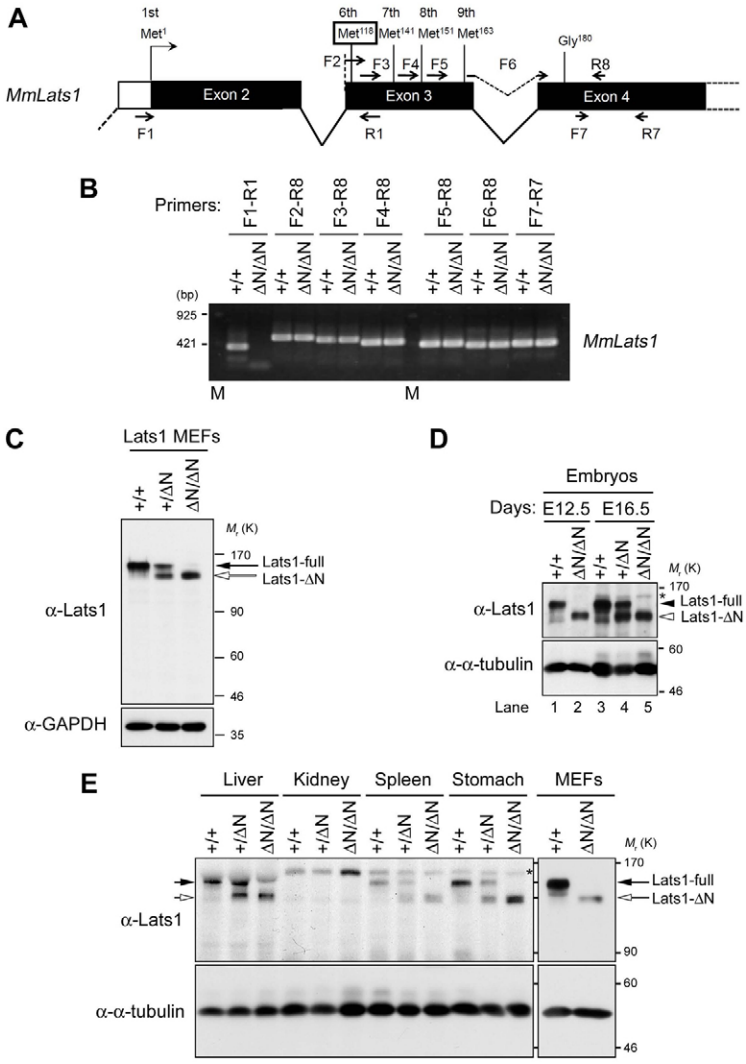

Fig. 1. Expression of N-terminally truncated Lats1 in *Lats1*$^{\Delta N/\Delta N}$ mice and MEFs. (**A**) Schematic representation of exons 2-4 of wild-type mouse *Lats1*. Boxes and kinked lines indicate exons and introns, respectively. Black boxes indicate coding exons. Arrows indicate primers for RT-PCR. The amino acid sequence surrounding Gly180 of mouse and human Lats1 is a putative epitope of anti-Lats1 monoclonal antibody (C66B5). (**B**) Expression of *Lats1* mRNA in *Lats1*$^{+/+}$ and *Lats1*$^{\Delta N/\Delta N}$ MEFs was analyzed by RT-PCR with the indicated seven sets of primer pairs. M, size marker. (**C**) Western blot analysis using cell lysates from *Lats1*$^{+/+}$, *Lats1*$^{+/\Delta N}$ and *Lats1*$^{\Delta N/\Delta N}$ MEFs. Full-length (black arrow) and truncated (ΔN, white arrow) Lats1 proteins were recognized by an anti-Lats1 monoclonal antibody (C66B5). GAPDH was analyzed as the loading control. The size of the Lats1-ΔN protein was ~1002–1042 aa. M_r(K), relative molecular mass (kDa). (**D**) Western blot analysis using homogenized lysates from *Lats1*$^{+/+}$, *Lats1*$^{+/\Delta N}$ and *Lats1*$^{\Delta N/\Delta N}$ mouse embryos at E12.5 and E16.5. The full-length and ΔN forms of Lats1 are indicated by black and white arrowheads, respectively. α-tubulin was used as a loading control. Asterisk indicates nonspecific bands. (**E**) Western blot analysis using homogenized lysates from the indicated tissues of *Lats1*$^{+/+}$, *Lats1*$^{+/\Delta N}$ and *Lats1*$^{\Delta N/\Delta N}$ adult mice. MEFs (top panel) are shown as a size control. The full-length and ΔN forms of Lats1 are indicated by black and white arrows, respectively. α-tubulin was used as a loading control.

examined the cell growth rate of *Lats1*$^{\Delta N/\Delta N}$ MEFs expressing the Lats1-ΔN protein with truncated LCD1. *Lats1*$^{\Delta N/\Delta N}$ MEFs did not exhibit a significant increase in growth rate (1.18 times), but *Lats1*$^{\Delta N/\Delta N}$ MEFs continued to grow, escaping from contact inhibition 5 days after the confluent stage (Fig. 2A,B, upper panels). By Day 12, *Lats1*$^{\Delta N/\Delta N}$ MEFs piled up (the increase in total cell number after 12 days was 2.2-fold) and formed foci that resembled cancer cells (Fig. 2B, lower panels), because their growth was not blocked by contact inhibition. Compared to *Lats1*$^{+/+}$ MEFs, more *Lats1*$^{\Delta N/\Delta N}$ MEFs were collected by microcentrifugation 8 days after contact inhibition (Fig. 2C). Consistent with these data, nuclear Orc2 (origin recognition complex 2; a DNA replication and cell growth marker) showed nuclear accumulation in *Lats1*$^{\Delta N/\Delta N}$ and *Lats1*$^{+/+}$ MEFs during cell growth (low cell density; supplementary material Fig. S3B, second panel) and *Lats1*$^{\Delta N/\Delta N}$ MEFs under conditions of high cell density (Fig. 6A, third panel from bottom), whereas it did not show nuclear accumulation in *Lats1*$^{+/+}$ MEFs during growth arrest (high cell density; Fig. 6A), suggesting that DNA replication was upregulated in *Lats1*$^{\Delta N/\Delta N}$ MEFs even under conditions of high cell density.

The anchorage-dependent growth effect was then examined in *Lats1*$^{\Delta N/\Delta N}$ MEFs in a soft-agar colony formation assay. *Lats1*$^{\Delta N/\Delta N}$ MEFs were horizontally dispersed and continued to grow with migration in soft agar, which prevented typical colony formation, whereas *Lats1*$^{+/+}$ MEFs did not grow or form colonies (Fig. 2D). This result is similar to that seen for tetraploid-derived epithelial cells with chromosomal abnormalities (Fujiwara et al., 2005).

We also investigated the abnormal growth of *Lats1*$^{\Delta N/\Delta N}$ MEFs using other 3D cell culture systems, such as NanoCulture Plates (NCPs) and 3D collagen gels (Mizushima et al., 2009). NCP is a synthetic resin film-bottom plate with a microscale structure that disturbs cell attachment to the matrix. When cultured on NCPs, *Lats1*$^{\Delta N/\Delta N}$ MEFs showed abnormally accelerated growth and spheroid formation, whereas *Lats1*$^{+/+}$ MEFs hardly grew (Fig. 2E). After incubation for 14 days, the number of living *Lats1*$^{\Delta N/\Delta N}$ MEFs in spheroids was three times greater than the number of *Lats1*$^{+/+}$ MEFs (Fig. 2F). *Lats1*$^{\Delta N/\Delta N}$ MEFs showed abnormally

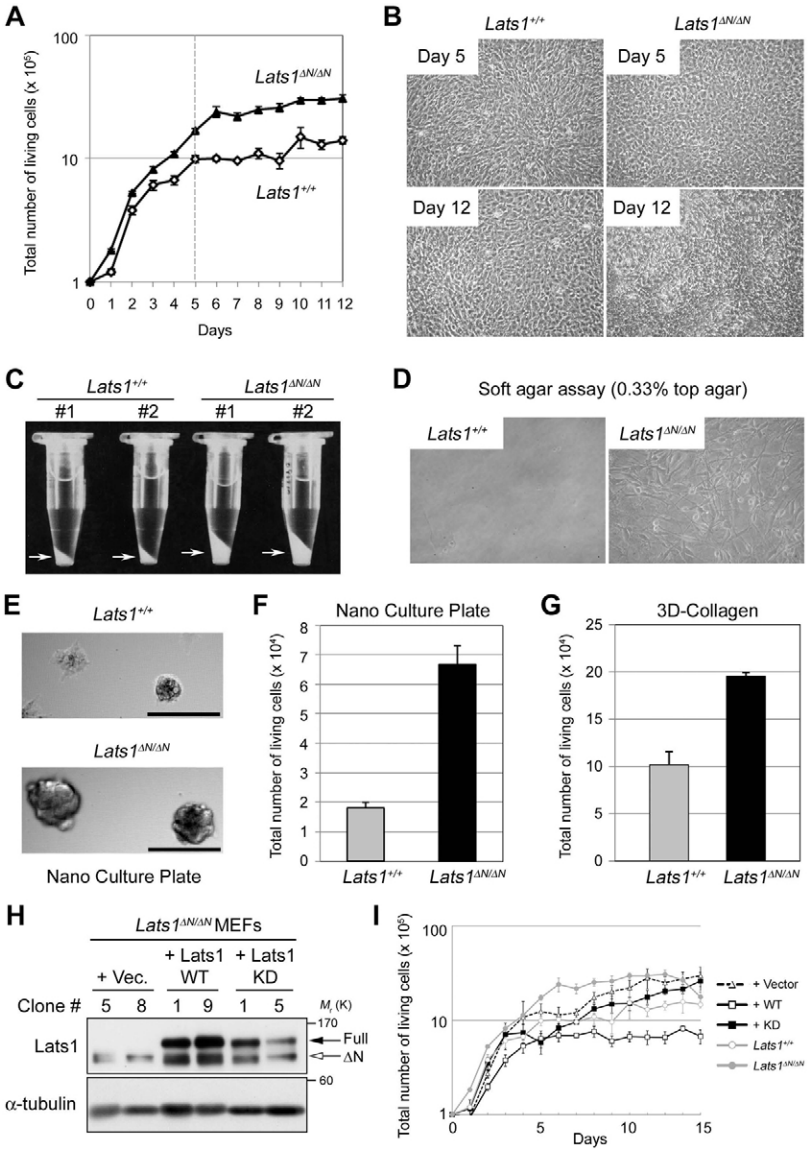

Fig. 2. *Lats1*$^{\Delta N/\Delta N}$ MEFs show anchorage-independent growth. (**A**) Cell growth curves of immortalized *Lats1*$^{+/+}$ (open diamonds) and *Lats1*$^{\Delta N/\Delta N}$ (closed triangles) MEFs. *Lats1*$^{+/+}$ MEFs were confluent at 5 days after plating (dashed line). Means and s.d. were derived from three individual experiments. (**B**) Morphology of *Lats1*$^{+/+}$ and *Lats1*$^{\Delta N/\Delta N}$ MEFs on days 5 and 12. (**C**) Representative pictures of *Lats1*$^{+/+}$ and *Lats1*$^{\Delta N/\Delta N}$ cell pellets (arrows) in centrifugation tubes. Cells were cultured for 8 days under contact inhibition and then scraped. Pellets were derived from two individual experiments (#1 and #2). (**D**) Soft-agar assay. The indicated MEFs were cultured in 0.33% top agar for 36 days. (**E**) 3D cell culture using NanoCulture Plates. *Lats1*$^{+/+}$ and *Lats1*$^{\Delta N/\Delta N}$ MEFs were plated at 1×10^4 cells and cultured on the plates for 14 days. Scale bars: 100 μm. (**F**,**G**) Number of *Lats1*$^{+/+}$ (gray bars) and *Lats1*$^{\Delta N/\Delta N}$ (black bars) MEFs growing on NanoCulture Plates (F) and in 3D-collagen gels (G). Means and s.d. were derived from three individual experiments. (**H**) Isolation of *Lats1*$^{\Delta N/\Delta N}$ MEF clones stably expressing full-length wild-type Lats1 (Lats1-WT), kinase- Lats1 (Lats1-KD) or vector alone. Cell lysates were prepared from two independent clones and analyzed by western blotting with the indicated antibodies. Exogenous full-length and endogenous ΔN forms of Lats1 are indicated by black and white arrows, respectively. (**I**) Growth curves of *Lats1*$^{\Delta N/\Delta N}$ MEF clones stably expressing full-length Lats1-WT (black lines and open squares), Lats1-KD (black lines and filled squares) and vector alone (gray dashed lines and triangles). Intact *Lats1*$^{+/+}$ (gray lines and open circles) and parental *Lats1*$^{\Delta N/\Delta N}$ (gray lines and filled circles) MEF are controls. Means and s.d. were derived from three individual experiments.

accelerated growth on 3D collagen gels (Fig. 2G). These results suggest that *Lats1*$^{\Delta N/\Delta N}$ MEFs exhibit abnormal cell growth and anchorage-independent growth, similar to tumor cells.

To confirm that the abnormal growth of *Lats1*$^{\Delta N/\Delta N}$ MEFs was due to the N-terminal deletion of Lats1, we isolated *Lats1*$^{\Delta N/\Delta N}$ MEF clones stably expressing full-length wild-type Lats1 (Lats1-WT), kinase-dead Lats1 (Lats1-KD), and vector alone (Fig. 2H). The abnormal growth of *Lats1*$^{\Delta N/\Delta N}$ MEFs was rescued by re-expression of full-length Lats1-WT, but not Lats1-KD or vector alone (Fig. 2I). This result indicates that the N-terminus and kinase activity of Lats1 are required for suppression of the abnormal growth of *Lats1*$^{\Delta N/\Delta N}$ MEFs. Lats1-KD overexpression likely dominantly inhibits Lats kinases and promotes cell growth as well as Lats2-KD (Nishioka et al., 2009). Thus, the abnormal growth of *Lats1*$^{\Delta N/\Delta N}$ MEFs is believed to be caused by the N-terminal deletion of Lats1, because the kinase activity of Lats1 was unaffected by its N-terminal deletion (see Fig. 6D).

N-terminally truncated Lats1 promotes tumorigenesis

To examine whether the abnormal growth of *Lats1*$^{\Delta N/\Delta N}$ MEFs contributed to tumorigenesis, *Lats1*$^{\Delta N/\Delta N}$ MEFs were injected subcutaneously into nude mice. As expected, all four of the *Lats1*$^{\Delta N/\Delta N}$ MEFs-injected mice produced tumors, whereas a *Lats1*$^{+/+}$ MEFs-injected mouse did not (Fig. 3A). Interestingly, the tumor size of *Lats1*$^{\Delta N/\Delta N}$ MEFs in nude mice increased very slowly (about two times slower than ordinary epithelial cancer cells) (Fig. 3B). Similar results were obtained in three independent experiments. These results suggest that the N-terminus of Lats1 is required for the suppression of tumorigenesis.

Lats1$^{\Delta N/\Delta N}$ MEFs exhibit centrosomal overduplication

Centrosomal aberrations and genomic instability are frequently observed in association with tumor progression in many human cancers (reviewed in Nigg, 2002; Nigg and Raff, 2009). Because Lats1 and Lats2 coordinately regulate mitosis by localizing to the centrosome and mitotic apparatus (Hirota et al., 2000; Toji et al., 2004; Yabuta et al., 2007; Yabuta et al., 2011), we investigated the impact of the N-terminal deletion of Lats1 on the centrosomal integrity by indirect immunofluorescence analysis using an antibody against γ-tubulin, a component of the PCM. The number of *Lats1*$^{\Delta N/\Delta N}$ cells with more than two γ-tubulin foci per single nucleus increased during interphase, whereas *Lats1*$^{+/+}$ MEFs normally possessed one or two γ-tubulin foci (Fig. 4A). Cells with more than two centrosomes were four times more abundant in *Lats1*$^{\Delta N/\Delta N}$ than in *Lats1*$^{+/+}$ MEFs (Fig. 4B).

The above finding raises the possibility that the N-terminal deletion of Lats1 leads to centrosomal overduplication (i.e. PCM is amplified with the centriole) or fragmentation (i.e. PCM, but not the centriole, is amplified). Immunofluorescence staining of centrin, a core component of the centriole, showed that all of the amplified γ-tubulin foci colocalized with centrin signals in a single *Lats1*$^{\Delta N/\Delta N}$ cell (Fig. 4C). Because γ-tubulin colocalized with centrin in 84% of all *Lats1*$^{\Delta N/\Delta N}$ MEFs, the phenomenon was due to centrosomal overduplication and not centrosomal fragmentation (Fig. 4D). Interestingly, centrosomal overduplication in *Lats1*$^{\Delta N/\Delta N}$ MEFs gradually diminished during successive passages up to PDL (population doubling level) 58, which indicates that centrosomal overduplication is suppressed by long-term passage in *Lats1*$^{\Delta N/\Delta N}$ MEFs (Fig. 4E,

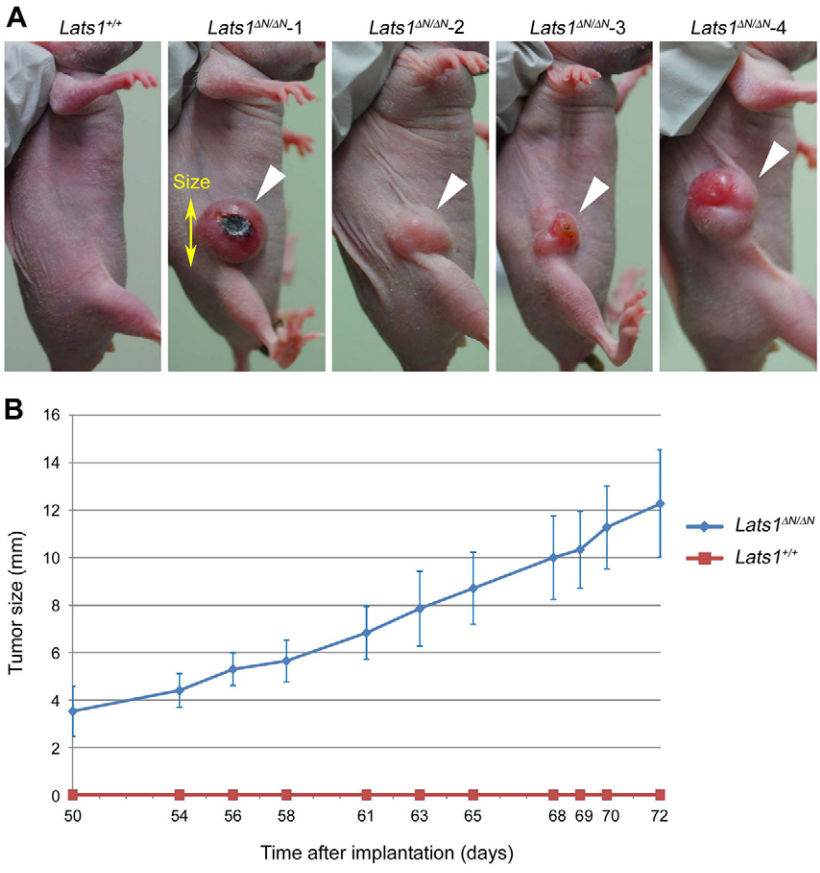

Fig. 3. *Lats1*$^{\Delta N/\Delta N}$ MEFs produce tumors when injected subcutaneously into nude mice. (**A**) Photographs of representative nude mice at 68 days after injection of *Lats1*$^{+/+}$ or *Lats1*$^{\Delta N/\Delta N}$ MEFs. White arrowheads indicate tumors at the injected site of 1×10^6 cells in nude mice. (**B**) Tumor size was measured at the indicated times. Means and s.d. were derived from the tumor sizes of four individual mice injected with *Lats1*$^{\Delta N/\Delta N}$ MEFs.

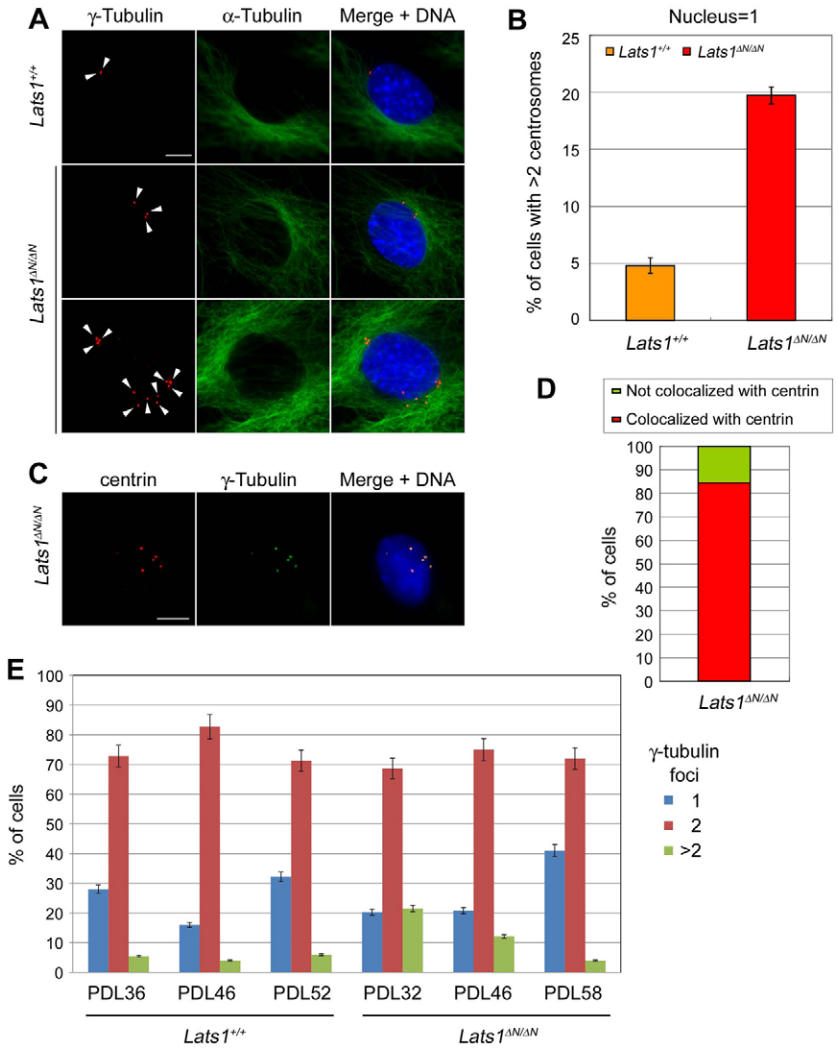

Fig. 4. *Lats1*$^{\Delta N/\Delta N}$ MEFs exhibit centrosomal overduplication. (**A**) *Lats1*$^{+/+}$ and *Lats1*$^{\Delta N/\Delta N}$ MEFs were immunostained with anti-γ-tubulin (as a PCM marker, red) and anti-α-tubulin (as a microtubule marker, green) antibodies and counterstained with Hoechst 33258 for DNA (blue). Arrowheads indicate increased γ-tubulin foci. (**B**) Frequencies of *Lats1*$^{+/+}$ (orange bar) and *Lats1*$^{\Delta N/\Delta N}$ (red bar) MEFs with more than two centrosomes and a nucleus. Data represent the means and s.d. of three independent experiments. (**C**) *Lats1*$^{\Delta N/\Delta N}$ MEFs were fixed with cold-methanol/acetone (1:1), immunostained with anti-centrin (as a centriole marker, red) and anti-γ-tubulin (green) antibodies and counterstained with Hoechst 33258 (DNA, blue). (**D**) Frequency of *Lats1*$^{\Delta N/\Delta N}$ MEFs with more than two γ-tubulin spots that colocalized (red bar) or not (green bar) with centrin. Data represent the averages of three independent experiments. (**E**) Percentage of cells with one, two or more than two centrosomes (γ-tubulin foci) at the indicated passages for *Lats1*$^{+/+}$ (PDL36, 46 and 52) and *Lats1*$^{\Delta N/\Delta N}$ (PDL32, 46 and 58) MEFs. Cells were immunostained with anti-γ-tubulin antibody as described above. Data represent the mean and s.d. of three independent experiments. In each experiment, >100 cells were counted. Scale bars: 10 μm.

green bars). Although centrosomal fragmentation was induced in *Lats2*$^{-/-}$ MEFs (Yabuta et al., 2007), a similar reduction was also observed after long-term passage of *Lats2*$^{-/-}$ MEFs (supplementary material Fig. S2). These results suggest that Lats1 negatively regulates centrosomal reduplication through the N-terminal region.

Lats1$^{\Delta N/\Delta N}$ MEFs exhibit chromosomal misalignment, multipolar spindle formation, chromosomal bridging and cytokinesis failure

Centrosomal aberration can promote abnormal spindle formation and chromosomal missegregation during mitosis (Nigg and Raff, 2009). We detected chromosomal misalignment (Fig. 5A), multipolar spindle formation (Fig. 5B), and chromosomal bridging (Fig. 5D) in *Lats1*$^{\Delta N/\Delta N}$ MEFs. By contrast, condensed chromosomes were properly aligned in the equatorial plane at metaphase in *Lats1*$^{+/+}$ MEFs and separated equally to the opposite poles at anaphase (Fig. 5A,D, upper panels). Misaligned chromosomes (46.3%) and multipolar spindles (23.1%) were conspicuous in metaphase in *Lats1*$^{\Delta N/\Delta N}$ MEFs (Fig. 5C). Chromosomal bridging was frequently (58.4%) observed at anaphase in *Lats1*$^{\Delta N/\Delta N}$ MEFs (Fig. 5E). We also observed cytokinesis failure in *Lats1*$^{\Delta N/\Delta N}$ MEFs, which led to a 4.3-fold increased number of multinucleated cells (Fig. 5F,G). These results suggest that loss of the N-terminal region of Lats1 causes chromosomal instability.

Yap protein stability is increased in *Lats1*$^{\Delta N/\Delta N}$ MEFs in a cell density independent manner

Once the Hippo pathway is activated in a cell density-dependent manner, activated Lats1/2 kinases phosphorylate at least five functional sites of the Yap transcriptional coactivator, thereby negatively regulating its oncogenic activity to promote cell proliferation even under conditions of cell contact inhibition (Zhao et al., 2007). The Lats1/2-mediated inhibitory mechanisms of the Yap protein are well-characterized, and involve two of the five phosphorylation sites on human Yap. In particular, (1) phosphorylation of Ser-127 (S127, corresponding to S112 of mouse Yap) leads to cytoplasmic retention of Yap through 14-3-3 binding (Zhao et al., 2007), and (2) phosphorylation of Ser-381 (S381, corresponding to S366 of mouse Yap) leads to phosphodegron-mediated degradation of Yap (Zhao et al., 2010).

Because *Lats1*$^{\Delta N/\Delta N}$ MEFs exhibited continued cell proliferation, even under conditions of high cell density and anchorage-independent growth, we investigated the impact of N-terminally truncated Lats1 on the phosphorylation and protein

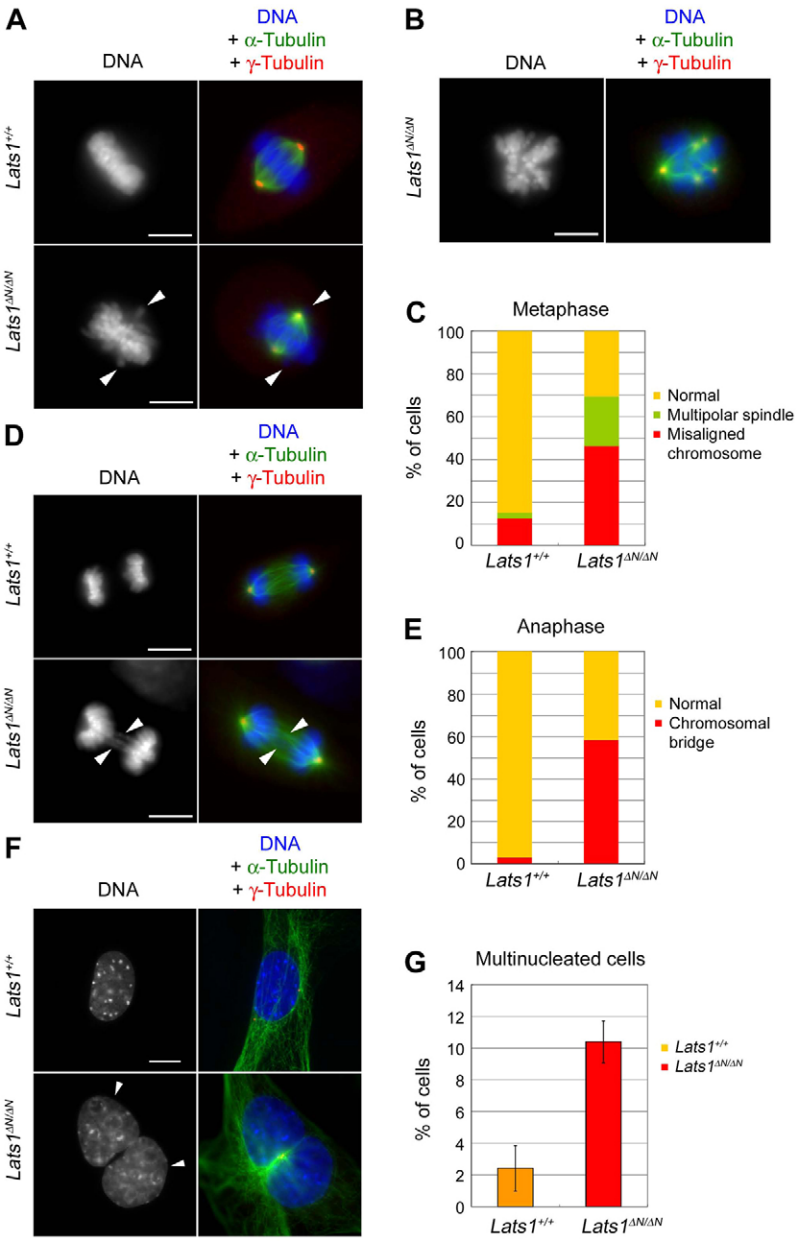

Fig. 5. *Lats1*$^{\Delta N/\Delta N}$ MEFs exhibit chromosomal misalignment, multipolar spindle formation, chromosome bridging and cytokinesis failure. (**A**,**B**,**D**,**F**) Immunofluorescent images show typical cells with misaligned chromosomes (A, arrowheads), multipolar spindles (B, chromosome bridging; D, arrowheads), and multinuclei (F, arrowheads) in *Lats1*$^{\Delta N/\Delta N}$ MEFs. *Lats1*$^{+/+}$ and *Lats1*$^{\Delta N/\Delta N}$ MEFs were stained with anti-γ-tubulin (red) and anti-α-tubulin antibodies (green) and counterstained with Hoechst for DNA (white or blue). Scale bars: 10 μm. (**C**) Number of cells at metaphase with normal (yellow bars), multipolar spindle (green bars) and misaligned chromosomes (red bars) in *Lats1*$^{+/+}$ and *Lats1*$^{\Delta N/\Delta N}$ MEFs. Data represent the average of three independent experiments. In each experiment, >40 metaphase cells were counted. (**E**) Number of cells at anaphase with normal (yellow bars) and bridging chromosomes (red bars) in *Lats1*$^{+/+}$ and *Lats1*$^{\Delta N/\Delta N}$ MEFs. Data represent the average of three independent experiments. In each experiment, >20 anaphase cells were counted. (**G**) Number of cells at interphase with bi- and multinuclei in *Lats1*$^{+/+}$ (yellow bar) and *Lats1*$^{\Delta N/\Delta N}$ (red bar) MEFs. Data represent the average of three independent experiments. In each experiment, >200 cells were counted. Error bars represent s.d.

stability of Yap. *Lats1*$^{+/+}$ and *Lats1*$^{\Delta N/\Delta N}$ MEFs were cultured under high cell density conditions, treated with cycloheximide (CHX) for a specified period, and fractionated into nuclear and cytoplasmic extracts. Consistent with previous reports using NIH3T3 cells and normal MEFs (Zhao et al., 2010), western blot analysis with a commercially available anti-Yap antibody [Yap (CST)] showed that most Yap resided in the cytoplasmic fraction. The Yap protein level was markedly decreased in *Lats1*$^{+/+}$ MEFs when *de novo* protein synthesis was blocked by CHX treatment (Fig. 6A, top panel, lanes 1–5). Unlike wild-type MEFs, Yap protein levels remained stable in the cytoplasm of *Lats1*$^{\Delta N/\Delta N}$ MEFs, even under high cell density conditions (Fig. 6A, top panel, lanes 11–15). Some protein was also detected in the nuclear fraction of *Lats1*$^{\Delta N/\Delta N}$ MEFs (Fig. 6A, top panel, lanes 16–20).

We confirmed these results using a novel anti-Yap polyclonal antibody [Yap (GS)] against an antigen different from that recognized by the available Yap (CST) antibody (see Materials and Methods). Both Yap antibodies recognized mouse and human Yap (supplementary material Fig. S3A). Similar results were obtained with the new Yap (GS) antibody (Fig. 6A, second panel). Notably, Yap proteins in *Lats1*$^{+/+}$ MEFs were unstable even at low cell density (although their instability was not as remarkable as that at high cell density), whereas Yap in *Lats1*$^{\Delta N/\Delta N}$ MEFs was relatively stable under the same condition (supplementary material Fig. S3B, top panel). These results suggest that, in *Lats1*$^{\Delta N/\Delta N}$ MEFs, the stability of Yap proteins is independent of cell density, and that most Yap protein is retained in the cytoplasm, with the exception of a small fraction that is localized to the nucleus.

The above findings suggest that the Yap-S112 phosphorylation (pS112) driving cytoplasmic retention may be defective in *Lats1*$^{\Delta N/\Delta N}$ MEFs. However, the phosphorylation level of cytoplasmic Yap-S112 was not significantly reduced in *Lats1*$^{\Delta N/\Delta N}$ MEFs compared with *Lats1*$^{+/+}$ MEFs, which was

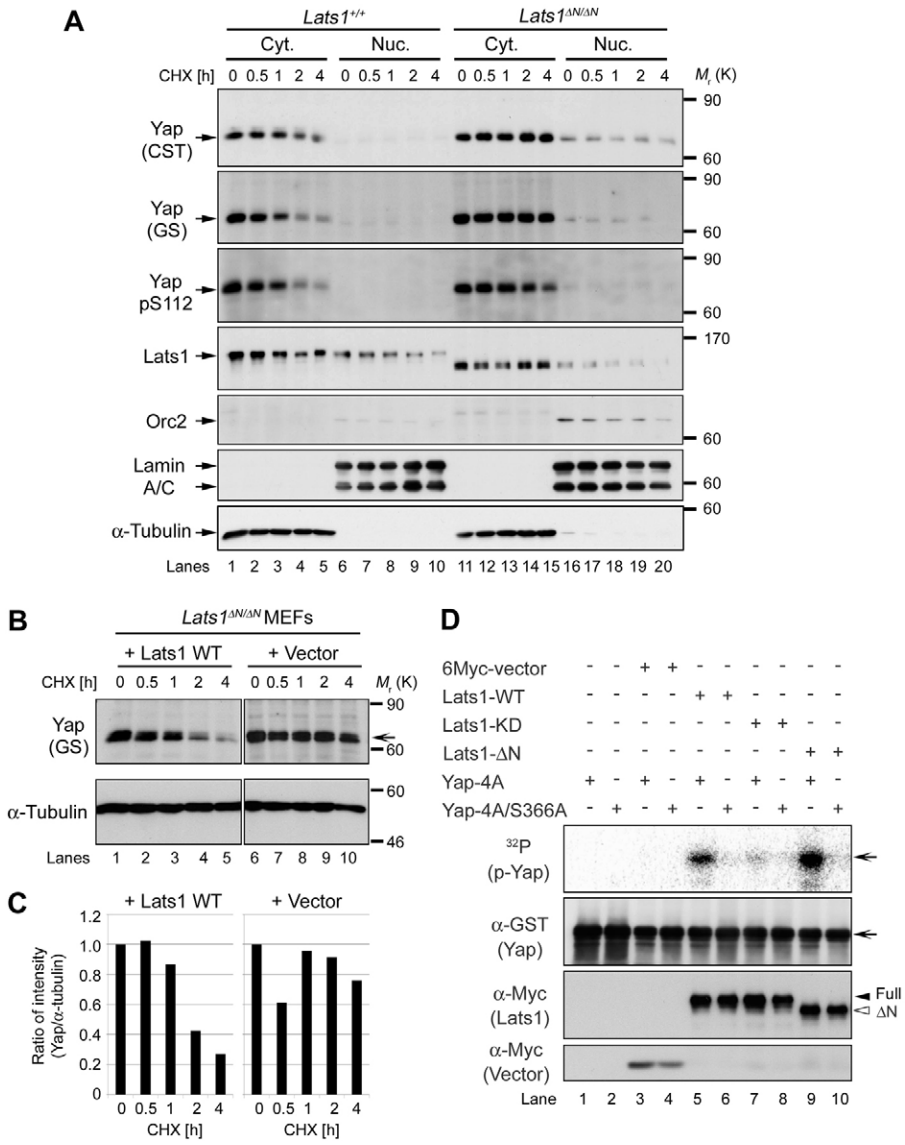

Fig. 6. Yap protein is stabilized in *Lats1*$^{\Delta N/\Delta N}$ MEFs. (**A**) *Lats1*$^{+/+}$ and *Lats1*$^{\Delta N/\Delta N}$ MEFs were cultured under high density (7 days after fully confluent), treated with cycloheximide (CHX) for the indicated period and separated into cytoplasmic (Cyt.) and nuclear (Nuc.) fractions. Fractionated lysates were analyzed by western blotting with the indicated antibodies. Lamin A/C and Orc2 are nuclear and DNA replication markers, respectively. α-tubulin was used as a cytoplasmic marker. (**B**) Stability of Yap protein in *Lats1*$^{\Delta N/\Delta N}$ MEFs was cancelled by adding back full-length Lats1. *Lats1*$^{\Delta N/\Delta N}$ MEF clones stably expressing full-length Lats1 wild-type (WT) or vector alone (pCX4bsr) were cultured under high density (7 days after fully confluent) and treated with CHX for the indicated period. Fractionated cytoplasmic lysates were analyzed by western blotting with the indicated antibodies. Arrow indicates endogenous Yap. (**C**) Ratio of each normalized Yap band intensity by α-tubulin band intensity. Data were obtained from B and measured with ImageJ software. (**D**) N-terminally truncated Lats1 potentially phosphorylates Yap at Ser366 as well as wild-type Lats1. *In vitro* Lats1-kinase assay with 6Myc-Lats1 immunoprecipitates (as kinases) and GST-Yap proteins (as substrates) in the presence of [γ-^{32}P]ATP (top panel). Reaction products were analyzed with the indicated antibodies. Lats1-ΔN (6M) is an N-terminally truncated Lats1 protein, which is translated from its own sixth internal methionine. Arrows, black arrowhead and white arrowhead show Yap, full-length Lats1 and Lats1-ΔN proteins, respectively.

correlated with the total Yap protein level (Fig. 6A, third panel). Interestingly, phosphorylation of Yap at S112 in *Lats2*$^{-/-}$ MEFs was almost similar to that in *Lats2*$^{+/+}$ MEFs (supplementary material Fig. S3C,D). The phosphorylation of S112 was decreased in *Lats2*$^{-/-}$ MEFs in which Lats1 expression was knocked-down by siRNA (supplementary material Fig. S3E). These results suggest that Lats1 and Lats2 can compensate for each other in respect to Yap-S112 phosphorylation, and that only by decreasing levels of both Lats proteins does pS112 decrease. Since Lats1-ΔN protein may possess sufficient kinase activity to phosphorylate Yap at S112 (supplementary material Fig. S3F), it is likely that the level of pS112 is similar in both *Lats1*$^{+/+}$ and *Lats1*$^{\Delta N/\Delta N}$ MEFs. In *Lats1*$^{\Delta N/\Delta N}$ MEFs, the stabilized Yap protein might be too abundant to be caught-up by S112-phosphorylation, which allows a portion of Yap to maintain its nuclear localization.

To confirm the contribution of the Lats1 N-terminus to Yap destabilization, we examined whether abnormal stabilization of Yap in *Lats1*$^{\Delta N/\Delta N}$ MEFs was rescued by re-expressing full-length Lats1. As expected, destabilization of the Yap protein was completely rescued by re-expressing full-length Lats1, but not vector alone, under high cell density conditions (Fig. 6B,C).

Because phosphorylation of Yap at S366 is essential for Yap destabilization, we examined whether Lats1-ΔN protein potentially possesses sufficient kinase activity to phosphorylate Yap on S366. *In vitro* kinase assays were performed using Lats1-immunoprecipitates (wild-type, kinase-dead and ΔN) as kinases and two kinds of mutated Yap as substrates. All of the Lats-mediated serine-phosphorylation sites of Yap (including S366) were substituted with alanine (4A/S366A), and four of the serine sites of Yap (excluding S366) were substituted with alanine (4A). Unexpectedly, immunoprecipitates of Lats1-ΔN incorporated radioactive phosphate into Yap-4A as well as into Yap-WT, but not into Yap-4A/S366A, and the incorporation was more efficient than that observed in Lats1-WT immunoprecipitates (Fig. 6D, top panel; supplementary material Fig. S3G). Consistent with this, Lats1-ΔN associated with Yap, and Mob1 interacted more efficiently with Lats1-ΔN than with Lats1-WT,

suggesting that the kinase activity of Lats1-ΔN is stronger than that of Lats1-WT (supplementary material Fig. S4A,B).

Together, these results suggest that Lats1-ΔN prevents Yap protein destabilization, although Lats1-ΔN is potentially able to interact with and phosphorylate Yap, thereby accelerating abnormal cell growth.

Lats1 N-terminal region and kinase activity are required for Lats2 expression in MEFs

Lats1$^{\Delta N/\Delta N}$ MEFs expressing Lats1-ΔN exhibited Yap protein stability. Because S112 and S366 of Yap are co-operatively phosphorylated by both Lats1/2 kinases, and Lats1-ΔN maintains its kinase activity, Lats2 kinase signaling may be responsible for Yap dysregulation in *Lats1*$^{\Delta N/\Delta N}$ MEFs. To address this hypothesis, we compared the expression profiles of genes, including Yap-targets and *Lats2*, in *Lats1*$^{+/+}$ and *Lats1*$^{\Delta N/\Delta N}$ MEFs under high and low cell density conditions using cDNA microarrays. Scatter plots showed that the mRNA level of *Ctgf* (cysteine-rich protein connective tissue growth factor), a Yap-target gene, was strongly repressed in *Lats1*$^{+/+}$ MEFs after changing to high cell density conditions (the ratio of high/low cell density showed a −60.9-fold change, $P=0.0346$), whereas the *Ctgf* level in *Lats1*$^{\Delta N/\Delta N}$ MEFs was only slightly repressed under high cell density conditions (the ratio of high/low cell density showed a −3.3-fold change, $P=0.0139$) (supplementary material Fig. S5A,B, black spots). These results indicate that the Yap activity inhibition at high cell density was prevented in *Lats1*$^{\Delta N/\Delta N}$ MEFs. Moreover, the aberrant transcription of *Ctgf* was apparently reduced by the expression of wt Lats1 under both low and high cell density conditions (supplementary material Fig. S5C,D), suggesting that expression of wt Lats1 rescued the aberrant transcription of *Ctgf* in *Lats1*$^{\Delta N/\Delta N}$ MEFs. However, the mRNA levels of other well-known Yap-induced genes, *Birc2* and *Birc5/survivin*, were not affected by differences in cell density or cell type (e.g. *Lats1*$^{+/+}$ or *Lats1*$^{\Delta N/\Delta N}$ MEFs) (supplementary material Fig. S5E,F), which is consistent with a previous report that *Birc2* and *Birc5* are not downregulated in the *Yap*$^{-/-}$ mouse embryo (Ota and Sasaki, 2008). Microarray analysis showed that the *Lats2* expression level was dramatically suppressed in *Lats1*$^{\Delta N/\Delta N}$ MEFs under both high and low cell density conditions compared with that in *Lats1*$^{+/+}$ MEFs (Fig. 7A,B). RT-PCR and western blot analyses revealed that *Lats2* expression was suppressed at the mRNA and protein levels in *Lats1*$^{\Delta N/\Delta N}$ MEFs, whereas their expression levels were normal in *Lats1*$^{+/+}$ MEFs (Fig. 7C,D). However, epigenetic analyses demonstrated that the contribution of epigenetic regulation to *Lats2* expression in *Lats1*$^{\Delta N/\Delta N}$ MEFs was minimal (supplementary material Fig. S6A–D).

Exogenous re-expression of full-length Lats1-WT suppressed Yap dysregulation under high cell density conditions and blocked aberrant overgrowth of *Lats1*$^{\Delta N/\Delta N}$ MEFs. If the downregulation of *Lats2* expression is responsible for these abnormal phenotypes of *Lats1*$^{\Delta N/\Delta N}$ MEFs, then the re-expression of full-length Lats1-WT may restore the *Lats2* expression level in *Lats1*$^{\Delta N/\Delta N}$ MEFs to the standard level. We examined the *Lats2* mRNA transcription level in *Lats1*$^{\Delta N/\Delta N}$ MEFs expressing full-length Lats1-WT by RT-PCR analysis. The *Lats2* expression level in *Lats1*$^{\Delta N/\Delta N}$ MEFs was completely rescued by re-expression of full-length Lats1-WT, but not Lats1-KD or vector alone (Fig. 7E,F). Western blot analysis revealed similar findings for the rescue of the Lats2 protein level (Fig. 7G; supplementary material; Fig. S4C). These results indicate that the N-terminus and kinase activity of Lats1 are required for transcription of *Lats2*, and suggest that Lats1 stringently regulates Lats2 expression. On the other hand, the expression of *Lats1* was not defective in *Lats2*$^{-/-}$ MEFs, suggesting that Lats1 expression is not regulated by Lats2 (supplementary material Fig. S5G). Proper expression levels of both Lats kinases may cooperatively regulate the precise subcellular localization and stability of Yap protein in MEFs. Consistent with our hypothesis, the deficiency of Lats2 kinase may be responsible for the abnormal stabilization of Yap in *Lats1*$^{\Delta N/\Delta N}$ MEFs.

Finally, we addressed why *Lats1*$^{\Delta N/\Delta N}$ mice (~14% of all born mice) often (but not always) successfully completed fetal development without early embryonic lethality and showed healthy growth, albeit with mild retardation until 4 weeks after birth, despite the abnormal cell growth and chromosomal instability of cultured MEFs from these mice. We examined the expression level of Lats2 protein in lysates from normally-developed *Lats1*$^{\Delta N/\Delta N}$ embryos at E16.5. Surprisingly, Lats2 protein was expressed in *Lats1*$^{\Delta N/\Delta N}$ embryos at the same level as that in *Lats1*$^{+/+}$ and *Lats1*$^{+/\Delta N}$ embryos (Fig. 7H), which indicated that Lats2 expression was differentially regulated by nonidentical mechanisms in embryos (and probably adult organs; Fig. 7I) and cultured MEFs. Therefore, it is likely that the low expression level of Lats2 through transcriptional dysregulation by N-terminally truncated Lats1 was responsible for the aberrant cell growth and chromosomal instability of *Lats1*$^{\Delta N/\Delta N}$ MEFs, whereas the Lats2 levels of *Lats1*$^{\Delta N/\Delta N}$ embryos or organs were virtually assured by the embryogenesis- or organ development-specific mechanisms mediated by the Hippo pathway, such as a linkage between regulation of cell polarity, cell adhesion, and cell growth (Feigin et al., 2009).

Discussion

Lats1 and Lats2 kinases are pivotal effectors of the Hippo pathway and proper mitotic progression, including mitotic exit and cytokinesis (Bothos et al., 2005; Yabuta et al., 2007; Pan, 2010). Using knockout mice expressing N-terminally truncated Lats1 protein (*Lats1*$^{\Delta N/\Delta N}$), we demonstrated that the N-terminal region (aa 1–117) of mouse Lats1 containing LCD1 was required for destabilization of the Yap protein via transcriptional regulation of Lats2 expression, in which anchorage-independent cell growth and tumorigenesis in a xenograft model were suppressed.

Our results allow us to propose a possible model for this process (supplementary material Fig. S7). In wild-type MEFs under Hippo pathway-activated conditions, Lats1 and Lats2 cooperatively phosphorylate both S127 and S381 (S112 and S366 in mouse, respectively) of almost all Yap protein without leakage, which promotes its cytoplasmic retention through 14-3-3 protein binding and polyubiquitylation-dependent degradation, prevents its nuclear accumulation, and represses the transcription of proliferation-related genes (e.g. *Ctgf*). In parallel, Lats1 might upregulate *Lats2* transcription by activating an uncharacterized transcription factor (X) through putative association with the N-terminal domain (LCD1) of Lats1 and Lats1-dependent phosphorylation(s) (P), thereby maintaining sufficient levels of functional Lats2 protein. On the other hand, N-terminally truncated Lats1 protein in *Lats1*$^{\Delta N/\Delta N}$ MEFs phosphorylates Yap on both sites, but cannot upregulate *Lats2* transcription owing to dissociation from the transcription factor

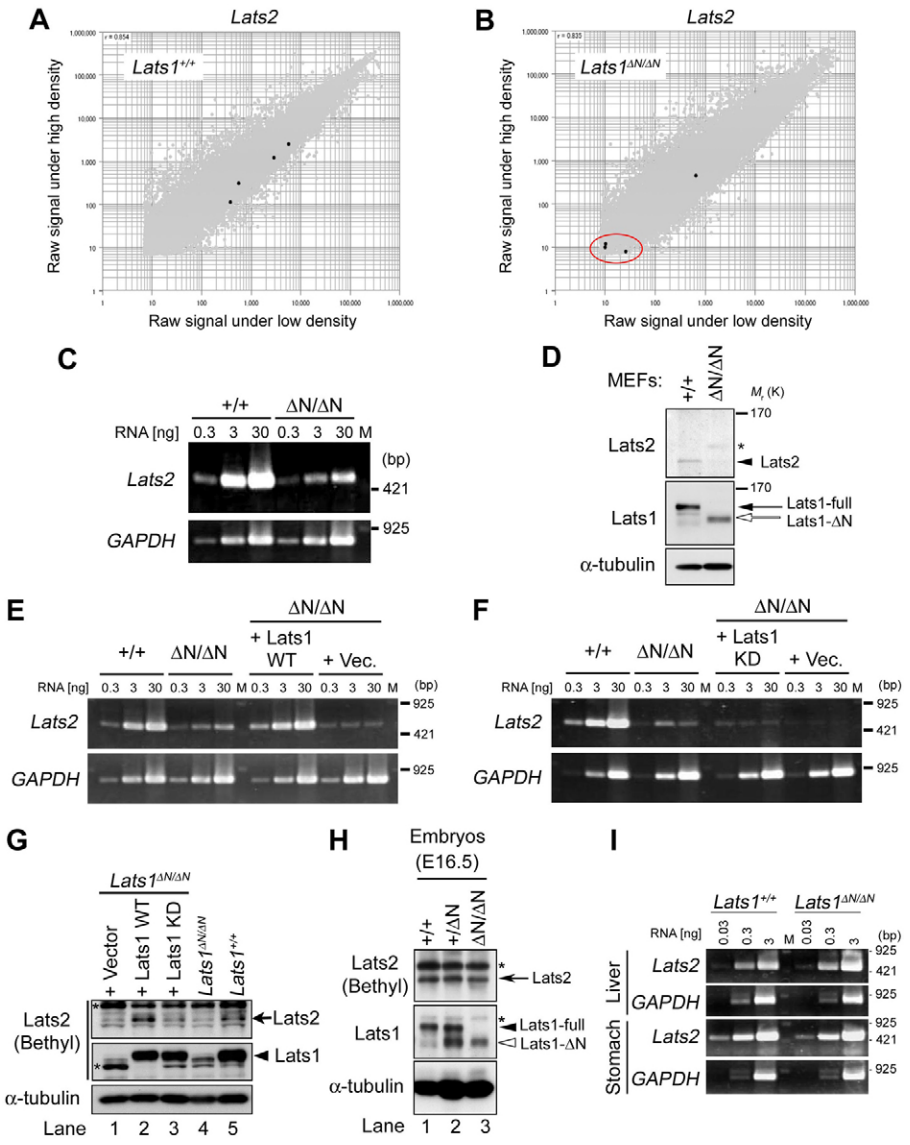

Fig. 7. N-terminal region of Lats1 is required for Lats2 expression in MEFs. (**A**,**B**) Scatter plots of DNA microarray data. Samples were obtained from *Lats1*$^{+/+}$ (A) and *Lats1*$^{\Delta N/\Delta N}$ (B) MEFs cultured at low (horizontal axis) or high density (vertical axis). The mRNA level of Lats2 is shown by black spots. Red circled dots are the signal from *Lats2* showing a negligible amount of expression. (**C**) Expression level of *Lats2* mRNA in *Lats1*$^{+/+}$ and *Lats1*$^{\Delta N/\Delta N}$ MEFs was analyzed by RT-PCR. The indicated amounts of total RNA from each MEF were used as templates. GAPDH is a loading control. M, size marker. (**D**) Expression level of Lats2 protein in *Lats1*$^{+/+}$ or *Lats1*$^{\Delta N/\Delta N}$ MEFs was detected by western blot analysis with the indicated antibodies. α-tubulin as used as a loading control. Asterisk indicates a nonspecific band. (**E**) *Lats2* mRNA level was rescued by re-expressing full-length Lats1 wild-type (WT) in *Lats1*$^{\Delta N/\Delta N}$ MEFs. RT-PCR analysis was performed as for C. *Lats1*$^{+/+}$ MEFs re-expressing vector alone (+ Vec.) were used as negative controls. (**F**) *Lats2* mRNA level was not rescued by re-expressing full-length Lats1-KD in *Lats1*$^{\Delta N/\Delta N}$ MEFs. RT-PCR analysis was performed as for E. (**G**) Lats2 protein level was rescued by re-expressing full-length Lats1-WT, but not Lats1-KD, in *Lats1*$^{\Delta N/\Delta N}$ MEFs. Lats2 and Lats1 were detected by western blot analysis with anti-Lats2 antibody (Bethyl). α-tubulin was used as a loading control. Asterisks indicate nonspecific bands. (**H**) Lats2 proteins were equally expressed in *Lats1*$^{+/+}$, *Lats1*$^{+/\Delta N}$ and *Lats1*$^{\Delta N/\Delta N}$ embryos at E16.5. Lats2 and Lats1 were detected by western blot analysis with anti-Lats2 (Bethyl) and anti-Lats1 (CST, C66B5) antibodies, respectively. α-tubulin was used as a loading control. Asterisk indicate nonspecific bands. (**I**) *Lats2* mRNA expression in liver and stomach was similar in *Lats1*$^{+/+}$ and *Lats1*$^{\Delta N/\Delta N}$ mice. RT-PCR analysis was performed as for C.

(X). Because cellular Lats2 protein levels are drastically reduced, it is impossible to maintain the inhibitory phosphorylation of Yap. Consequently, unphosphorylated (activated) Yap accumulates in the nucleus, where it promotes the transcription of proliferation-related genes and the cell growth, even under contact inhibition.

Our model reveals a linkage between Lats1 and Lats2 (at least in MEFs), i.e. Lats1 regulates the expression of Lats2. Lats1 overexpression might upregulate Lats2 protein levels, thereby having a synergetic effect on the negative regulation of Yap. Zhang et al. found that YAP-induced epithelial-mesenchymal transition (EMT) (including cell migration, soft-agar colony formation, and upregulation of the mesenchymal markers N-cadherin and fibronectin) in MCF10A breast cancer cells was more effectively suppressed by the enforced overexpression of Lats1 than by that of Lats2 alone, suggesting that Lats1 is the primary kinase that downregulates YAP-induced EMT (Zhang et al., 2008). However, because the phenotype of *Lats1*$^{\Delta N/\Delta N}$ MEFs is similar, but not identical, to that of *Lats2*$^{-/-}$ MEFs, Lats1 potentially possesses other individual functions that do not involve Lats2.

Although two conserved N-terminal domains (LCD1 and LCD2) of Lats2 reportedly play an important role in inhibiting NIH3T3/*v-ras* cell growth and soft-agar colony formation (Li et al., 2003), the molecular mechanism underlying this inhibition remains to be characterized. We demonstrated that the N-terminal region of Lats1, especially LCD1, was responsible for Lats2 expression in MEFs. Because it is unlikely that Lats1 aggressively contributes to the epigenetic regulation of *Lats2* expression (supplementary material Fig. S6), Lats1 might directly phosphorylate and regulate transcription factor(s) or modulator(s) through the binding of its LCD1. Lats kinases regulate some transcription factors, including p53, Taz, AR (androgen receptor), Snail1 and Yap (Powzaniuk et al., 2004; Lei et al., 2008; Aylon et al., 2010; Zhang et al., 2011). A recent study shows that ASPP1 promotes the nuclear translocation of Yap, which binds to the *LATS2* promoter and prevents p53-mediated *LATS2* expression in the human cancer cell lines, U2OS and HCT116

(Vigneron and Vousden, 2011). However, we were unable to find any putative p53-responsive elements in the mouse *Lats2* promoter. Moreover, depletion of Yap by siRNA did not restore *Lats2* expression in *Lats1*$^{\Delta N/\Delta N}$ MEFs (supplementary material Fig. S5H). Thus, even if the accumulated nuclear Yap binds to the mouse *Lats2* promoter and inhibits *Lats2* expression in MEFs (similar to human cancer cells) this activity would probably involve a transcription factor other than p53. Interestingly, the transcription factor FOXP3 binds to the human *LATS2* promoter and contributes to Yap phosphorylation upon *LATS2* expression in mammary epithelial cells, and *LATS2* expression is defective in human breast and prostate cancers (Li et al., 2011). However, if any transcription factors interact with the LCD1 of Lats1 or Lats2, they have not yet been identified.

In aggressive human breast cancers, the promoter regions of *LATS1* and *LATS2* are hypermethylated and their mRNA expression levels are downregulated (Takahashi et al., 2005). Because *Lats1*$^{\Delta N/\Delta N}$ MEFs can promote tumor progression in nude mice, we examined whether viable *Lats1*$^{\Delta N/\Delta N}$ mice develop spontaneous breast tumors. As expected, *Lats1*$^{\Delta N/\Delta N}$ mice did not develop spontaneous breast tumors (supplementary material Table S1). Moreover, *Lats1*$^{\Delta N/\Delta N}$ mice did not develop tumors in other organs, such as liver and stomach (supplementary material Fig. S1H; data not shown). Lats2 was highly expressed in healthy developing embryos (Fig. 7H) and adult organs (Fig. 7I) from *Lats1*$^{\Delta N/\Delta N}$ mice, but not in MEFs (Fig. 7D). Consistent with the observation in clinical human breast cancers, these results suggest that the downregulation of both Lats1 and Lats2 is significantly associated with tumor progression.

We found significant differences in *Lats2* expression levels between embryos and *Lats1*$^{\Delta N/\Delta N}$ MEFs (Fig. 7). However, the detailed mechanisms by which *Lats1*$^{\Delta N/\Delta N}$ embryos compensate for insufficient *Lats2* expression remain unknown. Cell type-dependent variations of the Hippo pathway have been observed between organs and cultured MEFs. For instance, Yap is efficiently inhibited by Lats1/2-mediated phosphorylation in MEFs, but is cooperatively inhibited by Lats1/2 and other unknown kinase(s) in the mouse liver (Zhou et al., 2009). Because the Hippo pathway regulates cell polarity, adhesion, and growth, the mechanisms of *Lats2* expression may show cell type-dependent variation through the Hippo pathway.

Taken together, our results suggest that Lats1 coordinates accurate cell growth control and chromosomal stability through *Lats2* expression and Yap stability in the Hippo pathway of MEFs.

Materials and Methods

Generation of the *Lats1* targeted allele

Gene targeting (supplementary material Fig. S1) and genotyping were performed as described previously (Yabuta et al., 2007).

Plasmids

Mouse kinase-dead Lats1 (MmLats1-KD; K733M), Lats2 (MmLats2-KD; K655A), and the N-terminally truncated MmLats1-ΔN (6M, aa 118–1129) were generated by a PCR-based method. These cDNAs were subcloned into the pCX4bsr vector (Akagi et al., 2003). Mouse YAP and human YAP were subcloned by PCR from cDNA libraries of mouse 10T1/2 cells and human uterine muscle, respectively. Mouse full-length YAP mutants (3A, 4A, 4A/S366A, 4A* and 4A*/S112A) were cloned into pGST6P.

Cell culture and transfection

Primary MEFs were obtained from mouse embryos at 12.5 days postcoitus and transfections were performed as described previously (Yabuta et al., 2007). Stably expressing clones were selected and maintained in the presence of 5 μg/ml of blasticidin S (Invivogen, San Diego, CA) for 2 weeks.

RT-PCR analysis

Total RNA was extracted from MEFs with an RNeasy Mini kit according to the manufacturer's instructions (Qiagen, Hilden, Germany). The cDNAs were synthesized from 3 μg (Fig. 1B; Fig. 7C,E,F,I; supplementary material Fig. S5G) or 0.3 μg (supplementary material Fig. S6) of RNA using the High-Capacity cDNA Archive Kit (Applied Biosystems, Foster City, CA). PCR was performed as described previously (Yabuta et al., 2007). The primers used here are shown in supplementary material Table S2.

Antibodies

Generation and purification of rabbit polyclonal antibody against the N-terminal region (aa 91–104) of human Yap2 [anti-Yap (GS)] were supported by GenScript Corporation (Piscataway, NJ).

Monoclonal (mAb) and polyclonal (pAb) antibodies against the following proteins were used: from Sigma, centrin pAb, γ-tubulin pAb/mAb, α-tubulin mAb, and FLAG-tag pAb/mAb; from Cell Signaling (Beverly, MA), Lats1 rabbit mAb (C66B5), YAP pAb, phospho-YAP (Ser127) pAb, and Lamin A/C mAb; from Bethyl Laboratories (Montgomery, TX), Lats2 pAb; from MBL (Nagoya, Japan), Myc-tag mAb (PL14) and pAb; from Research Diagnostics (Flanders, NJ), GAPDH mAb. Anti-Lats2 (LA-2) pAb, anti-GST mAb (4D8), and anti-Orc2 pAb were described previously (Yabuta et al., 2000; Yabuta et al., 2011).

Anchorage-independent growth assays

For the soft-agar colony formation assay, MEFs (1×10^3 cells/dish) were cultured in 4 ml of 0.33% top agar/MEF medium on 5 ml of 0.5% base agar/MEF medium in 6-cm culture dishes. After 36 days, cells were observed under a microscope (model IX71, Olympus). A 3D cell culture assay using collagen gels and NanoCulture plates (Scivax) was performed as described (Mizushima et al., 2009). Collected cells were counted in three independent experiments.

Tumorigenesis in nude mice

All animal experiments were performed with the approval of the Animal Experiments Committee of Osaka University (permit number: BikenA-H19-36-0 and BikenA-H19-37-0). BALB/c Slc-nu/nu female nude mice (4 weeks old; Japan SLC) were injected subcutaneously with 1×10^6 cells in 100 μl of MEF medium. Tumor growth was monitored every 2 or 3 days, and tumor size was measured using a caliper square.

Kinase assay, western blotting and immunofluorescence staining

The *in vitro* Lats1-kinase assay, preparation of whole cell lysates, western blotting, and indirect immunofluorescence staining were performed as described (Yabuta et al., 2007; Yabuta et al., 2011). Nuclear-cytoplasmic fractionation of MEFs was performed as described (Yabuta et al., 2000).

Microarray analysis

Total RNA was extracted from *Lats1*$^{+/+}$ and *Lats1*$^{\Delta N/\Delta N}$ MEFs with an RNeasy Minikit according to the manufacturer's instructions (Qiagen). Dye-swapped microarray analyses were performed as described (Ishii et al., 2005; Funato et al., 2010).

Statistical analysis

All data were expressed as the mean ± s.d. *P*-values were calculated by *t*-tests.

Acknowledgements

We thank Tomoya Hikita and Eisuke Mekada (Dept Cell Biology, R.I.M.D., Osaka University) for technical assistance with 3D collagen gel culture, Tsuyoshi Akagi (KAN Research Institute) for providing the pCX4bsr vector, and Patrick Hughes and Kathryn Kadash-Edmondson (Bioedit, Ltd) for critically reading the manuscript. We also thank Kana Ooi, Toshiya Hosomi, Souichi Nishihara, Mayumi Sugimoto, Azumi Fujimori (R.I.M.D., Osaka University) and Akiko Nagamori-Kawai (Genome Info. Res. Center, Osaka University) for technical help. The authors declare that they have no conflicts of interest.

Funding

This work was supported in part by Innovation Plaza Osaka of the Japan Science and Technology Agency (JST); and by Grants-in-aid for Scientific Research B [grant number 23370086 to H.N.] and C [grant number 22570185 to N.Y.] from the Ministry of Education, Culture, Sports, Science, and Technology of Japan.

Supplementary material available online at
http://jcs.biologists.org/lookup/suppl/doi:10.1242/jcs.113431/-/DC1

References

Abe, Y., Ohsugi, M., Haraguchi, K., Fujimoto, J. and Yamamoto, T. (2006). LATS2-Ajuba complex regulates gamma-tubulin recruitment to centrosomes and spindle organization during mitosis. *FEBS Lett.* **580**, 782-788.

Akagi, T., Sasai, K. and Hanafusa, H. (2003). Refractory nature of normal human diploid fibroblasts with respect to oncogene-mediated transformation. *Proc. Natl. Acad. Sci. USA* **100**, 13567-13572.

Aylon, Y., Michael, D., Shmueli, A., Yabuta, N., Nojima, H. and Oren, M. (2006). A positive feedback loop between the p53 and Lats2 tumor suppressors prevents tetraploidization. *Genes Dev.* **20**, 2687-2700.

Aylon, Y., Ofir-Rosenfeld, Y., Yabuta, N., Lapi, E., Nojima, H., Lu, X. and Oren, M. (2010). The Lats2 tumor suppressor augments p53-mediated apoptosis by promoting the nuclear proapoptotic function of ASPP1. *Genes Dev.* **24**, 2420-2429.

Boggiano, J. C. and Fehon, R. G. (2012). Growth control by committee: intercellular junctions, cell polarity, and the cytoskeleton regulate Hippo signaling. *Dev. Cell* **22**, 695-702.

Bothos, J., Tuttle, R. L., Ottey, M., Luca, F. C. and Halazonetis, T. D. (2005). Human LATS1 is a mitotic exit network kinase. *Cancer Res.* **65**, 6568-6575.

Chan, E. H., Nousiainen, M., Chalamalasetty, R. B., Schäfer, A., Nigg, E. A. and Silljé, H. H. (2005). The Ste20-like kinase Mst2 activates the human large tumor suppressor kinase Lats1. *Oncogene* **24**, 2076-2086.

Feigin, M. E. and Muthuswamy, S. K. (2009). Polarity proteins regulate mammalian cell-cell junctions and cancer pathogenesis. *Curr. Opin. Cell Biol.* **21**, 694-700.

Fujiwara, T., Bandi, M., Nitta, M., Ivanova, E. V., Bronson, R. T. and Pellman, D. (2005). Cytokinesis failure generating tetraploids promotes tumorigenesis in p53-null cells. *Nature* **437**, 1043-1047.

Funato, Y., Terabayashi, T., Sakamoto, R., Okuzaki, D., Ichise, H., Nojima, H., Yoshida, N. and Miki, H. (2010). Nucleoredoxin sustains Wnt/β-catenin signaling by retaining a pool of inactive dishevelled protein. *Curr. Biol.* **20**, 1945-1952.

Gordon, D. J., Resio, B. and Pellman, D. (2012). Causes and consequences of aneuploidy in cancer. *Nat. Rev. Genet.* **13**, 189-203.

Hanahan, D. and Weinberg, R. A. (2011). Hallmarks of cancer: the next generation. *Cell* **144**, 646-674.

Hergovich, A., Lamla, S., Nigg, E. A. and Hemmings, B. A. (2007). Centrosome-associated NDR kinase regulates centrosome duplication. *Mol. Cell* **25**, 625-634.

Hirota, T., Morisaki, T., Nishiyama, Y., Marumoto, T., Tada, K., Hara, T., Masuko, N., Inagaki, M., Hatakeyama, K. and Saya, H. (2000). Zyxin, a regulator of actin filament assembly, targets the mitotic apparatus by interacting with h-warts/LATS1 tumor suppressor. *J. Cell Biol.* **149**, 1073-1086.

Humbert, N., Navaratnam, N., Augert, A., Da Costa, M., Martien, S., Wang, J., Martinez, D., Abbadie, C., Carling, D., de Launoit, Y. et al. (2010). Regulation of ploidy and senescence by the AMPK-related kinase NUAK1. *EMBO J.* **29**, 376-386.

Iida, S., Hirota, T., Morisaki, T., Marumoto, T., Hara, T., Kuninaka, S., Honda, S., Kosai, K., Kawasuji, M., Pallas, D. C. et al. (2004). Tumor suppressor WARTS ensures genomic integrity by regulating both mitotic progression and G1 tetraploidy checkpoint function. *Oncogene* **23**, 5266-5274.

Ishii, T., Onda, H., Tanigawa, A., Ohshima, S., Fujiwara, H., Mima, T., Katada, Y., Deguchi, H., Suemura, M., Miyake, T. et al. (2006). Isolation and expression profiling of genes upregulated in the peripheral blood cells of systemic lupus erythematosus patients. *DNA Res.* **12**, 429-439.

Kamikubo, Y., Takaori-Kondo, A., Uchiyama, T. and Hori, T. (2003). Inhibition of cell growth by conditional expression of kpm, a human homologue of Drosophila warts/lats tumor suppressor. *J. Biol. Chem.* **278**, 17609-17614.

Ke, H., Pei, J., Ni, Z., Xia, H., Qi, H., Woods, T., Kelekar, A. and Tao, W. (2004). Putative tumor suppressor Lats2 induces apoptosis through downregulation of Bcl-2 and Bcl-x(L). *Exp. Cell Res.* **298**, 329-338.

Lei, Q. Y., Zhang, H., Zhao, B., Zha, Z. Y., Bai, F., Pei, X. H., Zhao, S., Xiong, Y. and Guan, K. L. (2008). TAZ promotes cell proliferation and epithelial-mesenchymal transition and is inhibited by the hippo pathway. *Mol. Cell. Biol.* **28**, 2426-2436.

Li, Y., Pei, J., Xia, H., Ke, H., Wang, H. and Tao, W. (2003). Lats2, a putative tumor suppressor, inhibits G1/S transition. *Oncogene* **22**, 4398-4405.

Li, W., Wang, L., Katoh, H., Liu, R., Zheng, P. and Liu, Y. (2011). Identification of a tumor suppressor relay between the FOXP3 and the Hippo pathways in breast and prostate cancers. *Cancer Res.* **71**, 2162-2171.

Liu, C. Y., Zha, Z. Y., Zhou, X., Zhang, H., Huang, W., Zhao, D., Li, T., Chan, S. W., Lim, C. J., Hong, W. et al. (2010). The hippo tumor pathway promotes TAZ degradation by phosphorylating a phosphodegron and recruiting the SCFbeta-TrCP E3 ligase. *J. Biol. Chem.* **285**, 37159-37169.

Matallanas, D., Romano, D., Al-Mulla, F., O'Neill, E., Al-Ali, W., Crespo, P., Doyle, B., Nixon, C., Sansom, O., Drosten, M. et al. (2011). Mutant K-Ras activation of the proapoptotic MST2 pathway is antagonized by wild-type K-Ras. *Mol. Cell* **44**, 893-906.

McPherson, J. P., Tamblyn, L., Elia, A., Migon, E., Shehabeldin, A., Matysiak-Zablocki, E., Lemmers, B., Salmena, L., Hakem, A., Fish, J. et al. (2004). Lats2/Kpm is required for embryonic development, proliferation control and genomic integrity. *EMBO J.* **23**, 3677-3688.

Mizushima, H., Wang, X., Miyamoto, S. and Mekada, E. (2009). Integrin signal masks growth-promotion activity of HB-EGF in monolayer cell cultures. *J. Cell Sci.* **122**, 4277-4286.

Morisaki, T., Hirota, T., Iida, S., Marumoto, T., Hara, T., Nishiyama, Y., Kawasuzi, M., Hiraoka, T., Mimori, T., Araki, N. et al. (2002). WARTS tumor suppressor is phosphorylated by Cdc2/cyclin B at spindle poles during mitosis. *FEBS Lett.* **529**, 319-324.

Nigg, E. A. (2002). Centrosome aberrations: cause or consequence of cancer progression? *Nat. Rev. Cancer* **2**, 815-825.

Nigg, E. A. and Raff, J. W. (2009). Centrioles, centrosomes, and cilia in health and disease. *Cell* **139**, 663-678.

Nishioka, N., Inoue, K., Adachi, K., Kiyonari, H., Ota, M., Ralston, A., Yabuta, N., Hirahara, S., Stephenson, R. O., Ogonuki, N. et al. (2009). The Hippo signaling pathway components Lats and Yap pattern Tead4 activity to distinguish mouse trophectoderm from inner cell mass. *Dev. Cell* **16**, 398-410.

Nishiyama, Y., Hirota, T., Morisaki, T., Hara, T., Marumoto, T., Iida, S., Makino, K., Yamamoto, H., Hiraoka, T., Kitamura, N. et al. (1999). A human homolog of Drosophila warts tumor suppressor, h-warts, localized to mitotic apparatus and specifically phosphorylated during mitosis. *FEBS Lett.* **459**, 159-165.

Okada, N., Yabuta, N., Suzuki, H., Aylon, Y., Oren, M. and Nojima, H. (2011). A novel Chk1/2-Lats2-14-3-3 signaling pathway regulates P-body formation in response to UV damage. *J. Cell Sci.* **124**, 57-67.

Ota, M. and Sasaki, H. (2008). Mammalian Tead proteins regulate cell proliferation and contact inhibition as transcriptional mediators of Hippo signaling. *Development* **135**, 4059-4069.

Pan, D. (2010). The hippo signaling pathway in development and cancer. *Dev. Cell* **19**, 491-505.

Powzaniuk, M., McElwee-Witmer, S., Vogel, R. L., Hayami, T., Rutledge, S. J., Chen, F., Harada, S., Schmidt, A., Rodan, G. A., Freedman, L. P. et al. (2004). The LATS2/KPM tumor suppressor is a negative regulator of the androgen receptor. *Mol. Endocrinol.* **18**, 2011-2023.

St John, M. A., Tao, W., Fei, X., Fukumoto, R., Carcangiu, M. L., Brownstein, D. G., Parlow, A. F., McGrath, J. and Xu, T. (1999). Mice deficient of Lats1 develop soft-tissue sarcomas, ovarian tumours and pituitary dysfunction. *Nat. Genet.* **21**, 182-186.

Takahashi, Y., Miyoshi, Y., Takahata, C., Irahara, N., Taguchi, T., Tamaki, Y. and Noguchi, S. (2005). Down-regulation of LATS1 and LATS2 mRNA expression by promoter hypermethylation and its association with biologically aggressive phenotype in human breast cancers. *Clin. Cancer Res.* **11**, 1380-1385.

Takahashi, A., Ohtani, N., Yamakoshi, K., Iida, S., Tahara, H., Nakayama, K., Nakayama, K. I., Ide, T., Saya, H. and Hara, E. (2006). Mitogenic signalling and the p16INK4a-Rb pathway cooperate to enforce irreversible cellular senescence. *Nat. Cell Biol.* **8**, 1291-1297.

Toji, S., Yabuta, N., Hosomi, T., Nishihara, S., Kobayashi, T., Suzuki, S., Tamai, K. and Nojima, H. (2004). The centrosomal protein Lats2 is a phosphorylation target of Aurora-A kinase. *Genes Cells* **9**, 383-397.

Vigneron, A. M. and Vousden, K. H. (2011). An indirect role for ASPP1 in limiting p53-dependent p21 expression and cellular senescence. *EMBO J.* **31**, 471-480.

Visser, S. and Yang, X. (2010). LATS tumor suppressor: a new governor of cellular homeostasis. *Cell Cycle* **9**, 3892-3903.

Xia, H., Qi, H., Li, Y., Pei, J., Barton, J., Blackstad, M., Xu, T. and Tao, W. (2002). LATS1 tumor suppressor regulates G2/M transition and apoptosis. *Oncogene* **21**, 1233-1241.

Yabuta, N., Fujii, T., Copeland, N. G., Gilbert, D. J., Jenkins, N. A., Nishiguchi, H., Endo, Y., Toji, S., Tanaka, H., Nishimune, Y. et al. (2000). Structure, expression, and chromosome mapping of LATS2, a mammalian homologue of the Drosophila tumor suppressor gene lats/warts. *Genomics* **63**, 263-270.

Yabuta, N., Okada, N., Ito, A., Hosomi, T., Nishihara, S., Sasayama, Y., Fujimori, A., Okuzaki, D., Zhao, H., Ikawa, M. et al. (2007). Lats2 is an essential mitotic regulator required for the coordination of cell division. *J. Biol. Chem.* **282**, 19259-19271.

Yabuta, N., Mukai, S., Okada, N., Aylon, Y. and Nojima, H. (2011). The tumor suppressor Lats2 is pivotal in Aurora A and Aurora B signaling during mitosis. *Cell Cycle* **10**, 2724-2736.

Yang, X., Li, D. M., Chen, W. and Xu, T. (2001). Human homologue of Drosophila lats, LATS1, negatively regulate growth by inducing G(2)/M arrest or apoptosis. *Oncogene* **20**, 6516-6523.

Zhang, J., Smolen, G. A. and Haber, D. A. (2008). Negative regulation of YAP by LATS1 underscores evolutionary conservation of the Drosophila Hippo pathway. *Cancer Res.* **68**, 2789-2794.

Zhang, K., Rodriguez-Aznar, E., Yabuta, N., Owen, R. J., Mingot, J. M., Nojima, H., Nieto, M. A. and Longmore, G. D. (2011). Lats2 kinase potentiates Snail1 activity by promoting nuclear retention upon phosphorylation. *EMBO J.* **31**, 29-43.

Zhao, B., Wei, X., Li, W., Udan, R. S., Yang, Q., Kim, J., Xie, J., Ikenoue, T., Yu, J., Li, L. et al. (2007). Inactivation of YAP oncoprotein by the Hippo pathway is involved in cell contact inhibition and tissue growth control. *Genes Dev.* **21**, 2747-2761.

Zhao, B., Ye, X., Yu, J., Li, L., Li, W., Li, S., Yu, J., Lin, J. D., Wang, C. Y., Chinnaiyan, A. M. et al. (2008). TEAD mediates YAP-dependent gene induction and growth control. *Genes Dev.* **22**, 1962-1971.

Zhao, B., Li, L., Tumaneng, K., Wang, C. Y. and Guan, K. L. (2010). A coordinated phosphorylation by Lats and CK1 regulates YAP stability through SCF(beta-TRCP). *Genes Dev.* **24**, 72-85.

Zhao, B., Tumaneng, K. and Guan, K. L. (2011). The Hippo pathway in organ size control, tissue regeneration and stem cell self-renewal. *Nat. Cell Biol.* **13**, 877-883.

Zhou, D., Conrad, C., Xia, F., Park, J. S., Payer, B., Yin, Y., Lauwers, G. Y., Thasler, W., Lee, J. T., Avruch, J. et al. (2009). Mst1 and Mst2 maintain hepatocyte quiescence and suppress hepatocellular carcinoma development through inactivation of the Yap1 oncogene. *Cancer Cell* **16**, 425-438.

Figure S1. Yabuta & Mukai *et al.*

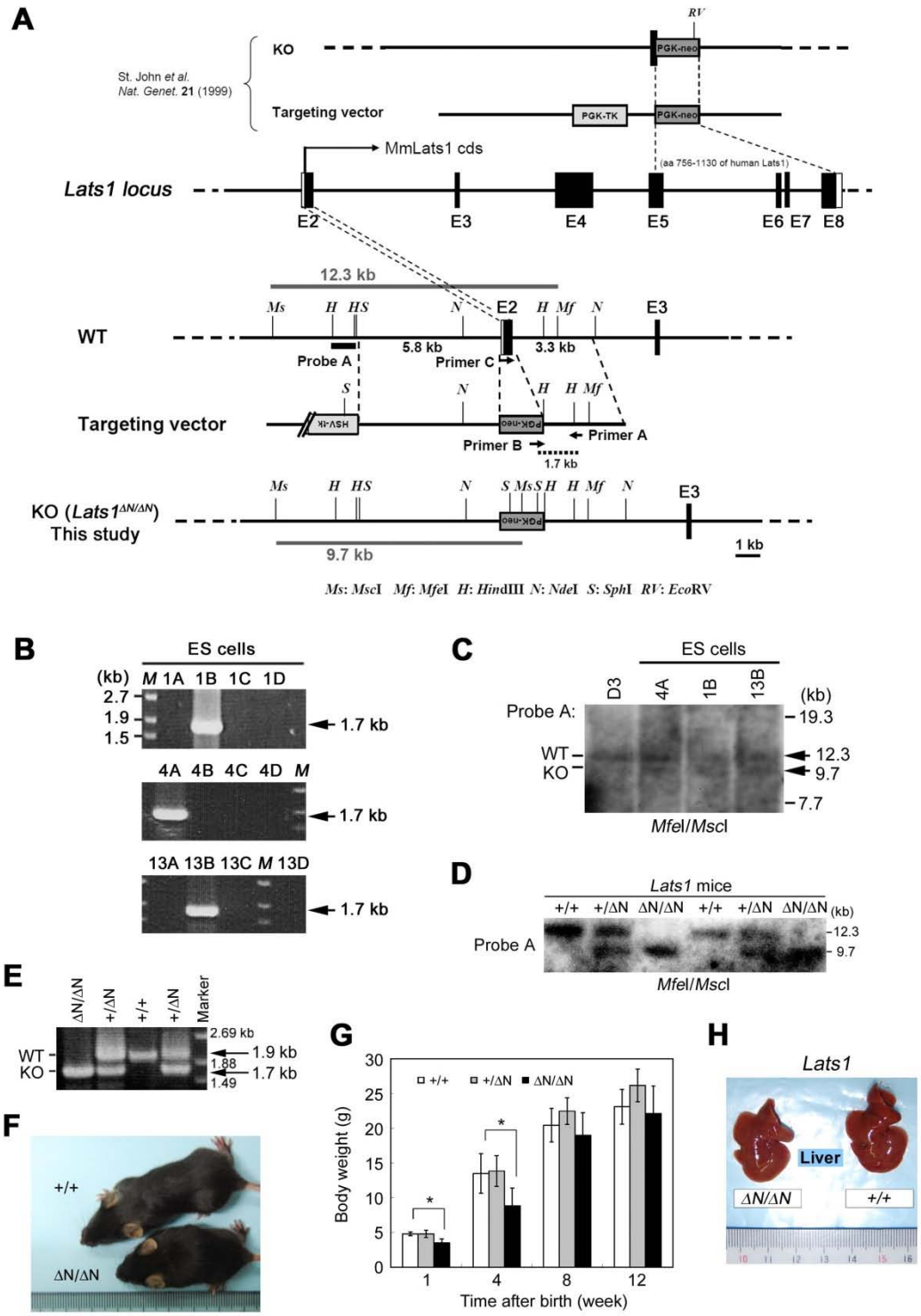

Fig. S1. Generation of *Lats1*$^{\Delta N/\Delta N}$ knockout mice.
(**A**) Schematic representation of the *Lats1* locus, targeting vector, and targeted locus (*Lats1*$^{\Delta N/\Delta N}$). To disrupt the N-terminal region of the *Lats1* gene, the neomycin selection cassette was replaced by the first coding exon (E2) in the targeting vector and *Lats1*$^{\Delta N/\Delta N}$. Black boxes indicate coding exons (E2–E8). Arrows indicate PCR primer positions. At the top is shown the targeting strategy used by St. John *et al.* (1999) for another *Lats1* knockout mouse, in which the protein sequence corresponding to 756–1130 of human Lats1 was removed. WT, wild-type; KO, knockout. (**B**) PCR analysis of genomic DNA from ES clones. Mutated clones (1B, 4A and 13B) were identified by the amplified products (1.7 kb) with primers A and B (shown in A). M, size maker. (**C**) Southern blot analysis of genomic DNA from ES clones. Genomic DNA was digested with *Mfe*I/*Msc*I. The WT (12.3 kb) and mutated fragment (9.7 kb) were identified by hybridization with probe A (shown in A). D3 is a negative control. (**D**) Southern blot analysis of genomic DNA from tails of offspring obtained from heterozygote intercrosses. Genomic DNA was digested with *Mfe*I/*Msc*I and hybridized with probe A. Fragments corresponding to the WT (12.3 kb) and KO (9.7 kb) are indicated. (**E**) Genomic PCR analysis of tails of offspring obtained from heterozygote intercrosses using a mixture of primers A, B, and C. Amplification products corresponding to the WT (1.9 kb) and KO (1.7 kb) alleles are indicated. (**F**) Representative picture of a *Lats1*$^{\Delta N/\Delta N}$ mouse (lower) with a *Lats1*$^{+/+}$ mouse (upper). (**G**) Body weights of *Lats1*$^{+/+}$ (white bars), *Lats1*$^{+/\Delta N}$ (gray bars), and *Lats1*$^{\Delta N/\Delta N}$ (black bars) mice from 1 to 12 weeks after birth. Data represent the average body weight of four offspring with each genotype. Error bars represent the SD. *$P < 0.001$. (**H**) The liver of *Lats1*$^{\Delta N/\Delta N}$ mice is normal in size and shows no tumor formation.

Figure S2. Yabuta & Mukai *et al.*

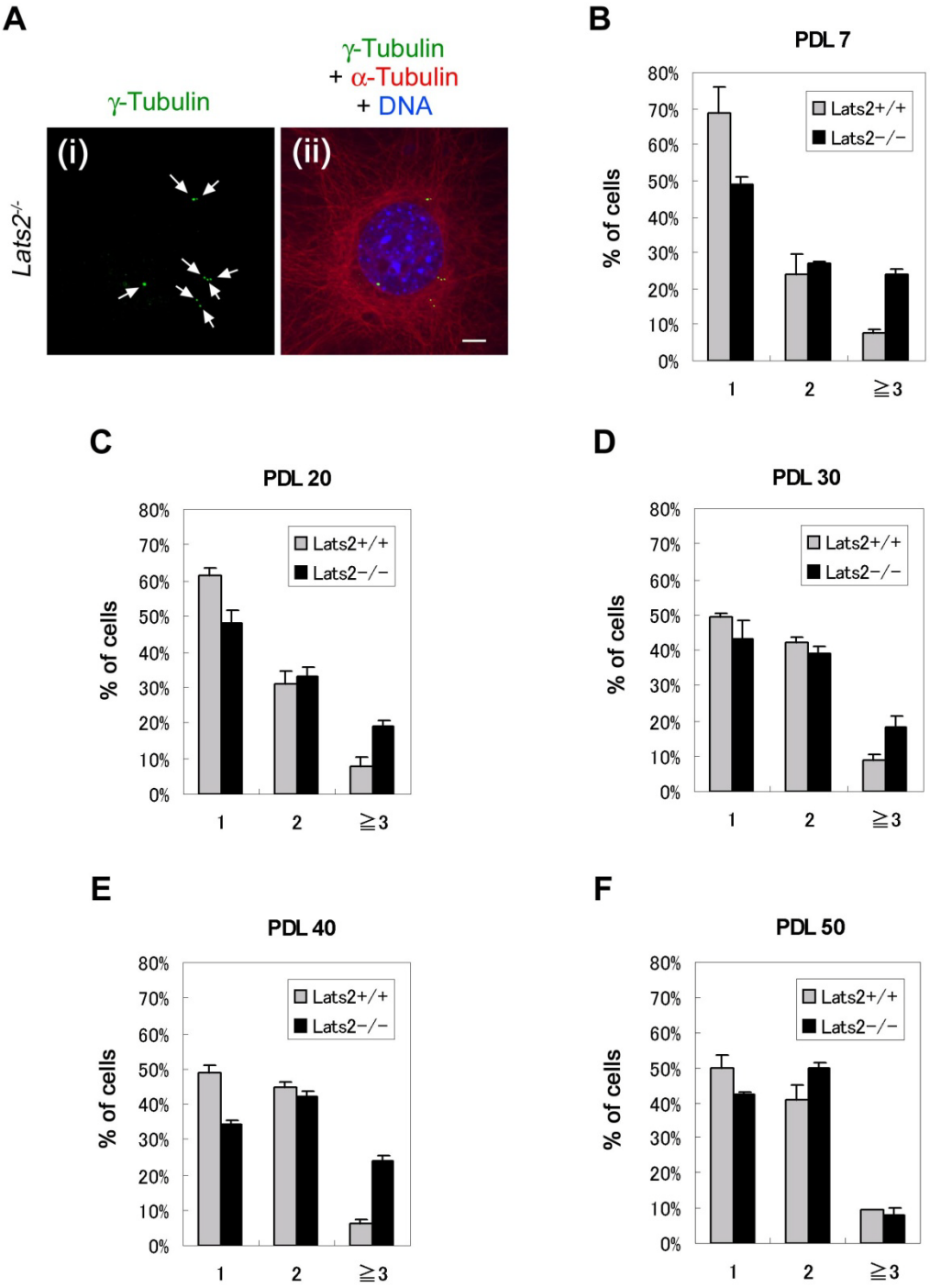

Fig. S2. Centrosomal fragmentation in *Lats2* knockout MEFs is suppressed in later passages.
(**A**, **B**) Immunofluorescence showing fragmented centrosomes in *Lats2*$^{-/-}$ MEFs during interphase. Cells were stained with anti-γ-tubulin (green) and anti-α-tubulin antibodies (red) and counterstained with Hoechst 33258 for DNA (blue). Arrows indicate fragmented centrosomes. Scale bars, 10 μm. (**C**–**G**) Percentage of cells with one, two, or more than two centrosomes in passages indicated (PDL7, 20, 30, 40, and 50) for MEFs of *Lats2*$^{+/+}$ (gray bars) and *Lats2*$^{-/-}$ (black bars). Cells were immunostained with an anti-γ-tubulin antibody as described above. Data represent the average of three independent experiments. In each experiment, >200 cells were counted. Error bars represent the SD.

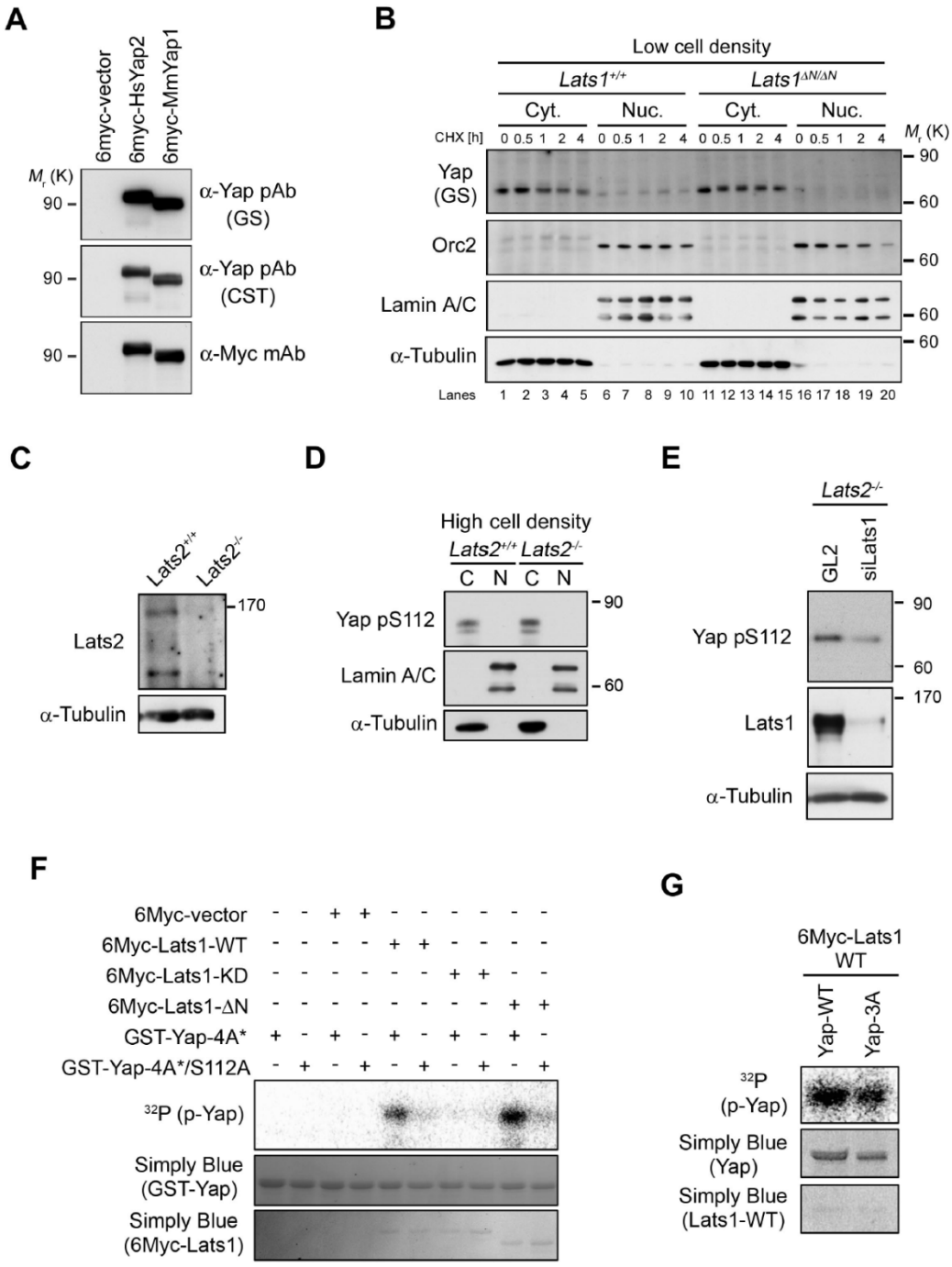

Fig. S3. Protein stability of Yap at low cell density, S112-phosphorylation of Yap, and quality of antibody against Yap. (**A**) A novel anti-Yap polyclonal antibody (GS) recognizes both human and mouse Yap equally as well as a commercially available anti-Yap antibody. 293T cells were transfected with 6Myc-tagged human Yap (HsYap2), mouse Yap (MmYap1), and 6Myc-vector alone. Transfected cells were Western blotted with anti-Yap (GS), commercially available anti-Yap (CST: Cell Signaling, #4912), and anti-Myc-tag antibodies. M_r(K), relative molecular mass (kDa). pAb and mAb indicate polyclonal and monoclonal antibodies, respectively. (**B**) *Lats1*$^{+/+}$ and *Lats1*$^{\Delta N/\Delta N}$ MEFs were cultured under low cell density, treated with cycloheximide (CHX) for the indicated period, and separated into cytoplasmic (Cyt.) and nuclear (Nuc.) fractions. Fractionated lysates were analyzed by Western blot analysis with the indicated antibodies. Lamin A/C and Orc2 are nuclear and DNA replication markers, respectively. α-tubulin was used as a cytoplasmic marker. M_r(K), relative molecular mass (kDa). (**C**) Western blotting of the cell lysates from *Lats2*$^{+/+}$ and *Lats2*$^{-/-}$ MEFs with anti-Lats2 (LA2) and α-tubulin antibodies. (**D**) Western blot analysis of cytoplasmic (C) and nuclear (N) extracts from *Lats2*$^{+/+}$ and *Lats2*$^{-/-}$ MEFs with the pS112-Yap antibody. (**E**) *Lats2*$^{-/-}$ MEFs were transfected with the indicated siRNA duplex and Lipofectamine 2000 (Invitrogen). GL2 is a negative control. Western blot analysis of the lysates with the pS112-Yap antibody. (**F**) In vitro Lats1-kinase assay with 6Myc-Lats1 immunoprecipitates (as kinases) and GST-Yap proteins (as substrates) in the presence of [γ-^{32}P]ATP (top panel). All of the Lats-mediated serine-phosphorylation sites of Yap (including S112) were substituted with alanine (4A*/S112A), and four of the serine sites of Yap (excluding S112) were substituted with alanine (4A*). Simply Blue (Invitrogen) staining shows the loading control. (**G**) In vitro Lats1-kinase assay with 6Myc-Lats1 immunoprecipitates (as kinases) and two kinds of GST-Yap proteins (Yap-WT and Yap-3A; as substrates) in the presence of [γ-^{32}P]ATP (top panel). Yap-3A: S46A, S94A, and S149A.

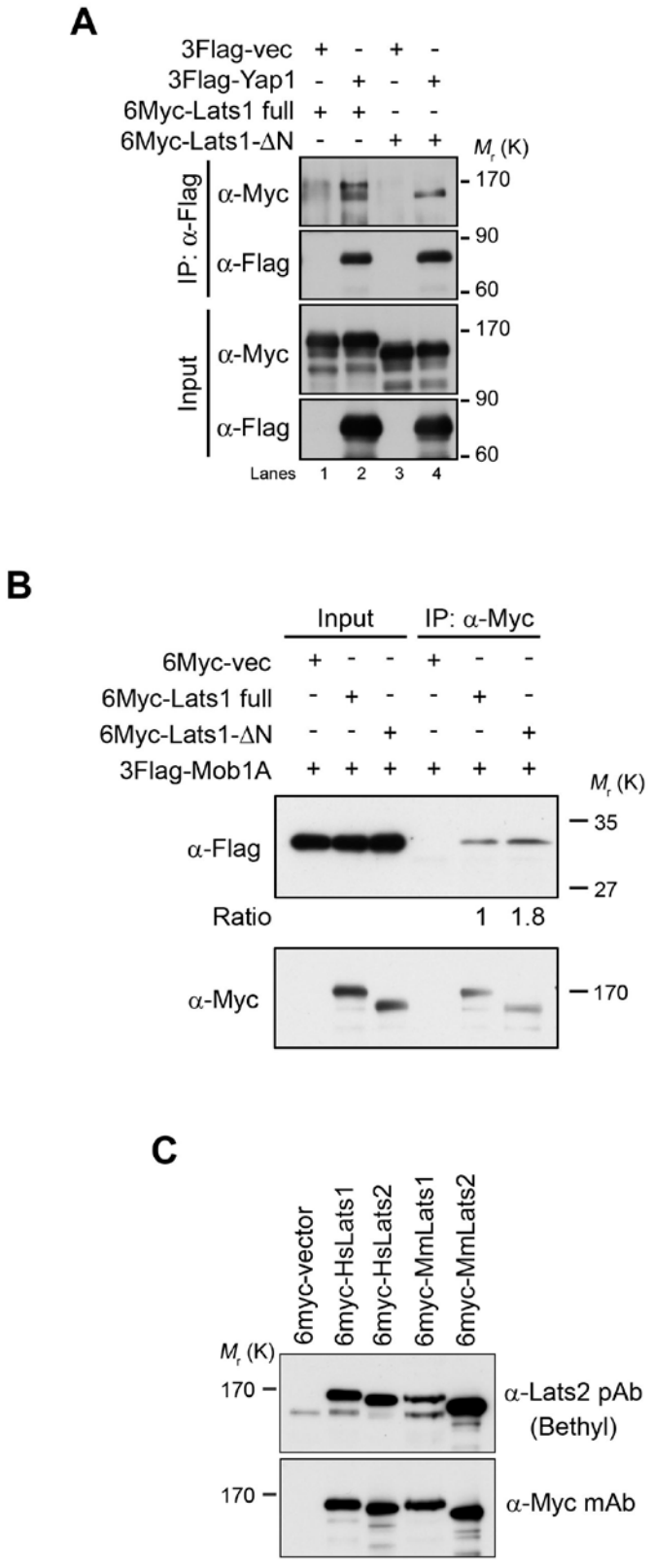

Fig. S4. Quality of the antibody against Lats2 and interaction of Lats1-ΔN with Yap and Mob1.
(**A**) Lats1-ΔN, as well as full length Lats1-WT, associates with Yap. 293T cells were cotransfected with 6Myc-Lats1 (full length or ΔN) and 3Flag-Yap. The lysate was subjected to immunoprecipitation (IP) with anti-Flag antibody, followed by Western blot analysis with anti-Myc and anti-Flag antibodies. M_r(K), relative molecular mass (kDa). (**B**) Mob1A interacts more efficiently with Lats1-ΔN than with Lats1-WT. 293T cells were cotransfected with 6Myc-Lats1 (full length or ΔN) and 3Flag-Mob1A. The lysate was subjected to immunoprecipitation (IP) with anti-Myc antibody, followed by Western blotting with anti-Myc and anti-Flag antibodies. (**C**) A commercially available anti-Lats2 antibody cross-reacts with human and mouse Lats1. 293T cells were transfected with 6Myc-tagged human (Hs) and mouse (Mm) Lats1 and Lats2, followed by Western blot analysis with a commercially available anti-Lats2 antibody (Bethyl Laboratories, # A300-479A) and an anti-Myc antibody.

Figure S5. Yabuta & Mukai *et al.*

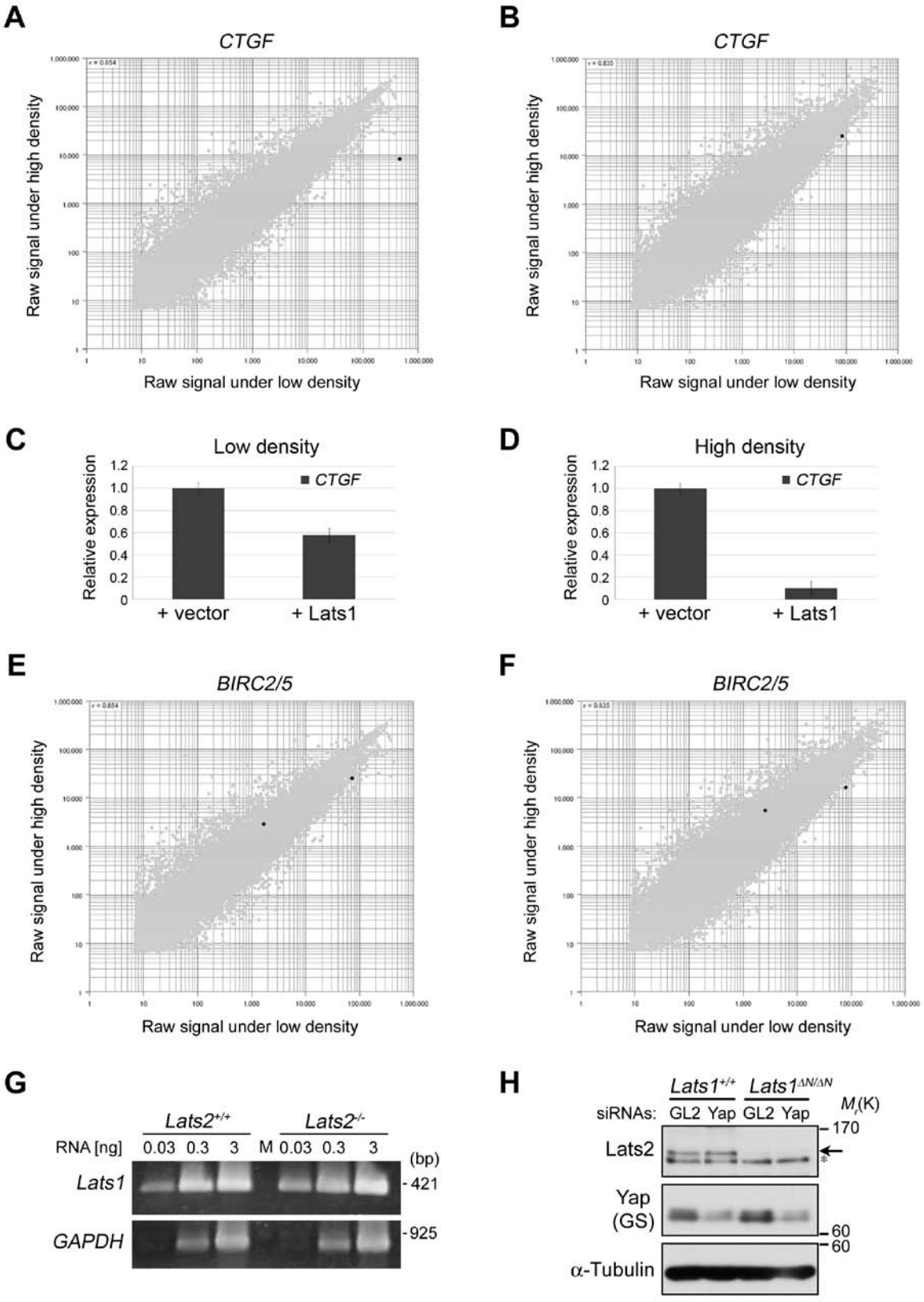

Fig. S5. Expression of two YAP-target genes, *Ctgf* and *Birc2/5*, in *Lats1*$^{+/+}$ and *Lats1*$^{\Delta N/\Delta N}$ MEFs. Scatter plots of DNA microarray data. RNA samples were obtained from *Lats1*$^{+/+}$ (**A**, **E**) and *Lats1*$^{\Delta N/\Delta N}$ (**B**, **F**) MEFs that were cultured at low (horizontal axis) or high density (vertical axis). The mRNA levels of *Ctgf* (**A**, **B**) and *Birc2/5* (**E**, **F**) are shown by black spots. (**C, D**) Total RNA was extracted from pCX4bsr-vec/*Lats1*$^{\Delta N/\Delta N}$ and pCX4bsr-Lats1full/ *Lats1*$^{\Delta N/\Delta N}$ cells under conditions of low (**C**) or high (**D**) cell density. The cDNAs were synthesized from 3 μg of RNA. To examine the mRNA levels of *Ctgf* in these cells, real-time PCR was performed on an Applied Biosystems 7900 HT FAST Real-Time PCR System using 20 ng cDNA and a master mix of SYBR Premix ExTaq II (Tli RNaseH Plus) (TaKaRa Bio, Japan). All quantifications were normalized by using the endogenous level of *GAPDH*. (**G**) Expression of *Lats1* mRNA in *Lats2*$^{+/+}$ and *Lats2*$^{-/-}$ MEFs was confirmed by RT-PCR analysis. *GAPDH* was analyzed as a loading control. M, size marker. (**H**) Expression of Lats2 in Yap-depleted *Lats1*$^{\Delta N/\Delta N}$ MEFs was examined by Western blot analysis with Lats2 antibody (black arrow). GL2 is a negative control. * indicates a nonspecific band.

Figure S6. Yabuta & Mukai *et al.*

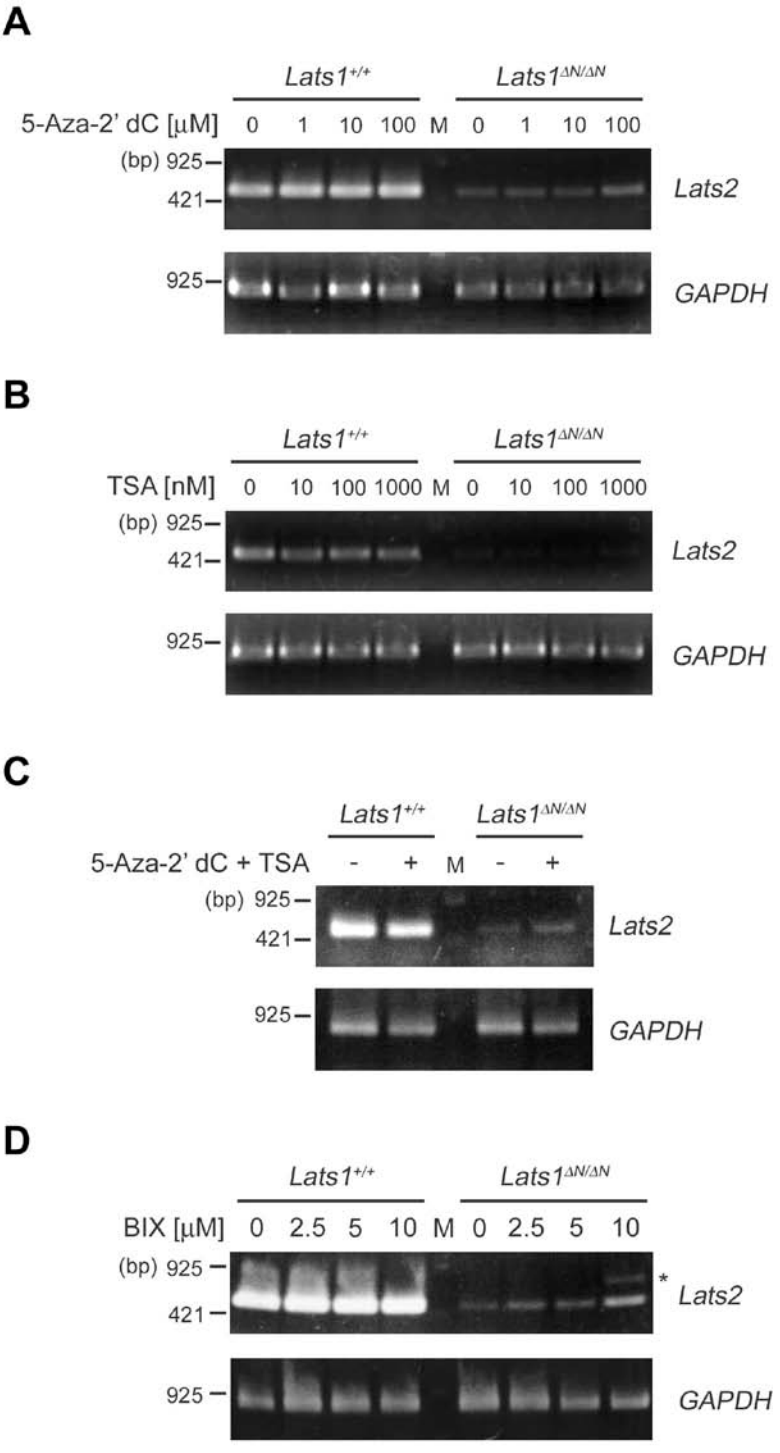

Fig. S6. DNA or histone methylation and histone deacetylation show little effect on the downregulation of Lats2 mRNA in *Lats1*$^{\Delta N/\Delta N}$ MEFs.

(**A**–**D**) Expression of *Lats2* mRNA was confirmed by RT-PCR analysis. *GAPDH* was analyzed as a loading control. (**A**) *Lats2* transcription level is slightly restored in *Lats1*$^{\Delta N/\Delta N}$ MEFs by treatment with a high concentration of a DNA methylation inhibitor, 5-Aza-2'-deoxycytidine (5-Aza-2'-dC). *Lats1*$^{+/+}$ and *Lats1*$^{\Delta N/\Delta N}$ MEFs were treated with 5-Aza-2'-dC, at the indicated concentration for 24 h. (**B**) No recovery of *Lats2* transcription is observed in TSA (trichostatin A, a histone deacetylation inhibitor)-treated *Lats1*$^{\Delta N/\Delta N}$ MEFs. MEFs were treated with TSA at the indicated concentration for 24 hours. (**C**) The *Lats2* transcription level is slightly restored in *Lats1*$^{\Delta N/\Delta N}$ MEFs by treatment with both 5-aza-2'-dC and TSA. MEFs were sequentially treated with (+) or without (-) 5-Aza-2'-dC (10 μM) for 24 hours and TSA (100 nM) for 24 hours. (**D**) The *Lats2* transcription level is slightly restored in *Lats1*$^{\Delta N/\Delta N}$ MEFs by treatment with a high concentration of a histone methylation inhibitor, BIX-01294 (BIX). MEFs were treated with BIX at the indicated concentration for 24 hours. * indicates unexpected bands. M, size marker.

Figure S7. Yabuta & Mukai *et al*.

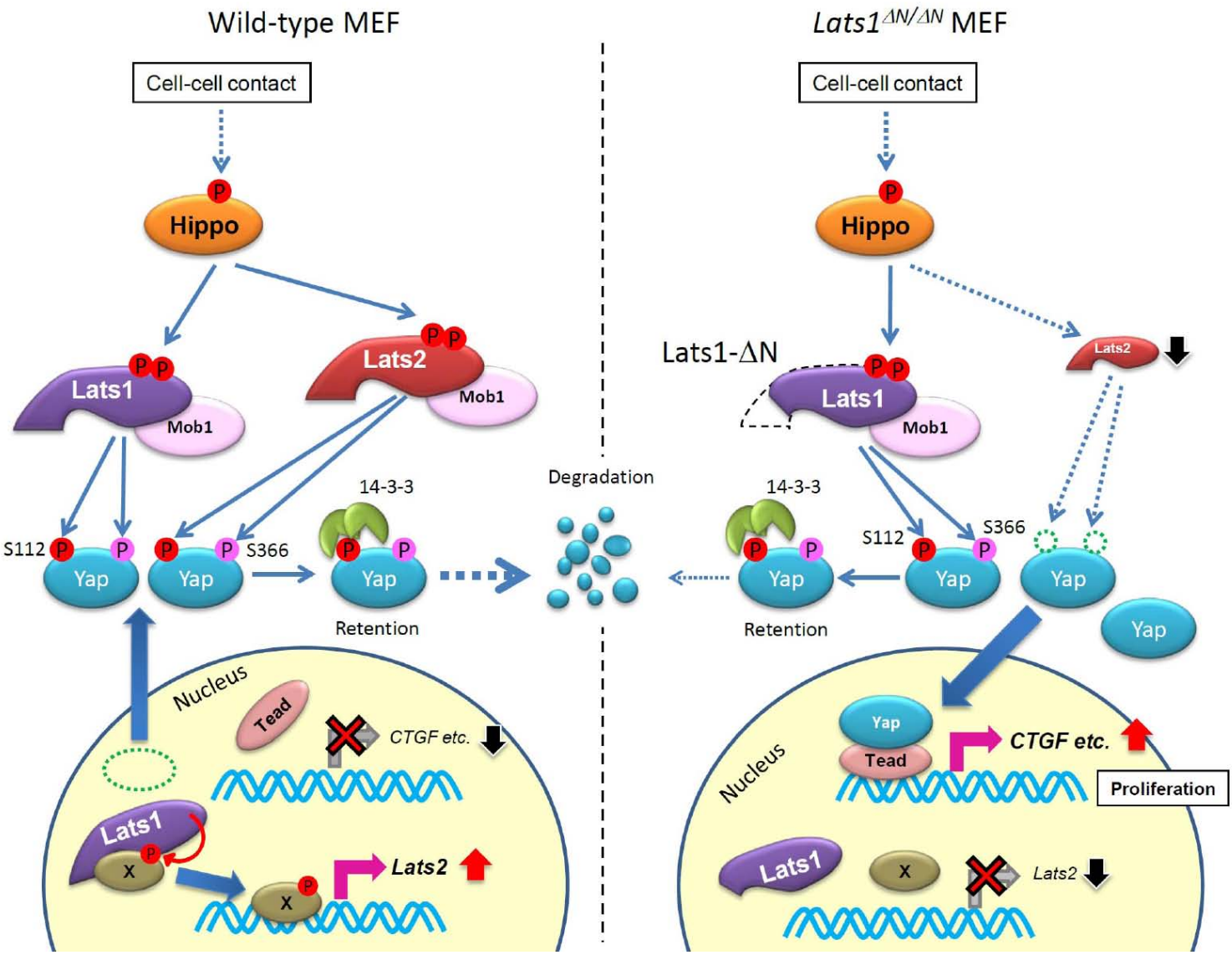

Fig. S7. Speculative model for the role of Lats1 N-terminal region and kinase activity in the Hippo pathway. See Discussion section for details.

Table S1. No spontaneous breast tumors in *Lats1*$^{\Delta N/\Delta N}$ mice

Incidence of spontaneous breast tumors in Lats1 mice

Genotype	Age (weeks)	Mouse number	Tumor incidence (%)
Lats1$^{+/+}$	0-24	16	0/16 (0%)
	25-48	14	0/14 (0%)
	49-72	114	0/114 (0%)
Lats1$^{+/\Delta N}$	0-24	19	0/19 (0%)
	25-48	45	0/45 (0%)
	49-72	80	0/80 (0%)
Lats1$^{\Delta N/\Delta N}$	0-24	2	0/2 (0%)
	25-48	6	0/6 (0%)
	49-72	36	0/36 (0%)

Supplementary Table S2. Yabuta & Mukai *et al.*

Primer name	DNA sequences
(A)	
Primer A (Lats1 KO con3)	5′-aaactggcaccaggttaatggg-3′
Primer B (KS conB)	5′-aggtcgacggtatcgataagc-3′
Primer C (Lats1-check2)	5′-ggtacagacagatgaggcctaagac-3′
Probe A-Fw	5′-cgcggatccaggttgagtgtaatctagcaagg-3′
Probe A-Rv	5′-ggaattctggaaatgtaagcttatcttctagg-3′
(B)	
F1	5′-gtgaaaagccagaagggtac-3′
R1	5′-cggcttctatgcttctgttattgg-3′
F2	5′-gacatggttattcaagctcttc-3′
F3	5′-ccaataacagaagcatagaagccg-3′
F4	5′-gagttaccaagaccctcgtcg-3′
F5	5′-ctgccaggcctattaatgcc-3′
F6	5′-gaaaccaggaaatgtgcaac-3′
F7	5′-caagcaatggacagagagtg-3′
R7	5′-ggtgcacgataaaatcagac-3′
R8	5′-ggggagattcgggagattac-3′
Lats2-exon5-F	5′-agcaggagcagatgaggaag-3′
Lats2-exon5-R	5′-agtgcagaggccaaaatctg-3′
mGAPDH-F	5′-tcaccatcttccaggagcgag-3′
mGAPDH-R	5′-gctgtagccgtattcattgtc-3′
MmCtgf-qRT-Fw	5′-gggcctcttctgcgatttc-3′
MmCtgf-qRT-Rv	5′-atccaggcaagtgcattggta-3′
(C)	
AscI-HsYap2-s	5′-tatggcgcgcctatggatcccgggcagcagccg-3′
HsYap2-PflMI-as	5′-tatgaattcccaagaggtggtcttgttcttatgg-3′
HsYap2-PflMI-s	5′-tatggcgcgccccacctcttggctagacccaaggc-3′
HsYap2-NotI-as	5′-tatggtaccgcggccgcctataaccatgtaagaaagctttc-3′
AscI-MmYap1-s	5′- tatggcgcgcctatggagcccgcgcaacagccg-3′
MmYap1-EcoRI-as	5′-tatgaattcatcagcgtctggggcaccg-3′
MmYap1-EcoRI-s	5′-tatggcgcgccgaattctgcctcaggacctcttcc-3′
MmYap1-NotI-as	5′-tatggtaccgcggccgcctataaccacgtgagaaagctttc-3′
BamAsc-mLats1-M1	5′-tatggatccggcgcgcctgccaccatgaagaggggtgaaaagccag-3′
BamAsc-mLats1-M6	5′-tatggatccggcgcgcctgccaccatggttattcaagctcttcag-3′
mLats1-705-NotXho	5′-tatctcgagcggccgcgttcactctctgtccattgcttg-3′
mLats1-K733M-F	5′-gtatgcaacaatgactcttcgaaag-3′
mLats1-K733M-R	5′-ctttcgaagagtcattgttgcatac-3′
mLats2-K655A-s	5′-acgccatggcgactctcaggaag-3′
mLats2-K655A-as	5′-tgagagtcgccatggcgtacag-3′
Long arm-AscI (lats1.ko.L1-2)	5′-tgctctagaggcgcgccaacccaggacttttcatatactaagc-3′
Long arm-XbaI (lats1.ko.L2-2-AS)	5′-tgctctagatagagttattaatgaagcagttcg-3′
Short arm-BamHI (lats1.ko.S3-2)	5′-cgcggatcctttcttttgagaggacttacctg-3′
Short arm-NotI (lats1.ko.S4.7-2-AS)	5′-tatggatccgcggccgctgagtcctctggaagagtagc-3′
(D)	
GL2	5′-cguacgcggaauacuucgadTdT-3′
	5′-ucgaaguauuccgcguacgdTdT-3′
siMmLats1-1414	5′-gcaagucacucugcuaauudTdT-3′
	5′-aauuagcagagugacuugcdTdT-3′
siMmYap1-909	5′-gcgguugaaacaacaggaauudTdT-3′
	5′-aauuccuguuguuucaaccgcdTdT-3′

Table S2 Sequences of oligonucleotide primers used in genotyping (**A**), RT-PCR (**B**), and plasmid construction (**C**), and sequences of siRNA duplexes (**D**).